

<sup>1</sup> **Pixels to pachyderms: Dual framework testing  
for Predicting Elephant Habitat Suitability**

<sup>3</sup> Harin Aiyanna C. R.<sup>1</sup>, Brooke Friswold<sup>2,3,4</sup>, Antoinette van de Water<sup>4,5</sup>,  
<sup>4</sup> Francesco Pirotti<sup>1,6</sup>

<sup>5</sup> <sup>1</sup> TESAF Department of Land, Environment, Agriculture, and Forestry, University of  
<sup>6</sup> Padova, Padova 35020, Veneto, Italy

<sup>7</sup> <sup>2</sup> Department of Wildlife Ecology and Conservation, University of Florida, Gainesville  
<sup>8</sup> 32611, Florida, USA

<sup>9</sup> <sup>3</sup> Conservation Ecology Program, King Mongkut's University of Technology Thonburi,  
<sup>10</sup> Bangkok 10150, Thailand

<sup>11</sup> <sup>4</sup> Bring The Elephant Home, Steven Butendiekplateau 130, 3581 GS Utrecht, The  
<sup>12</sup> Netherlands

<sup>13</sup> <sup>5</sup> School of Life Sciences, University of KwaZulu-Natal, Scottsville 32009, South Africa

<sup>14</sup> <sup>6</sup> CIRGEO Interdepartmental Research Center of Geomatics, University of Padova,  
<sup>15</sup> Legnaro 35020, Veneto, Italy

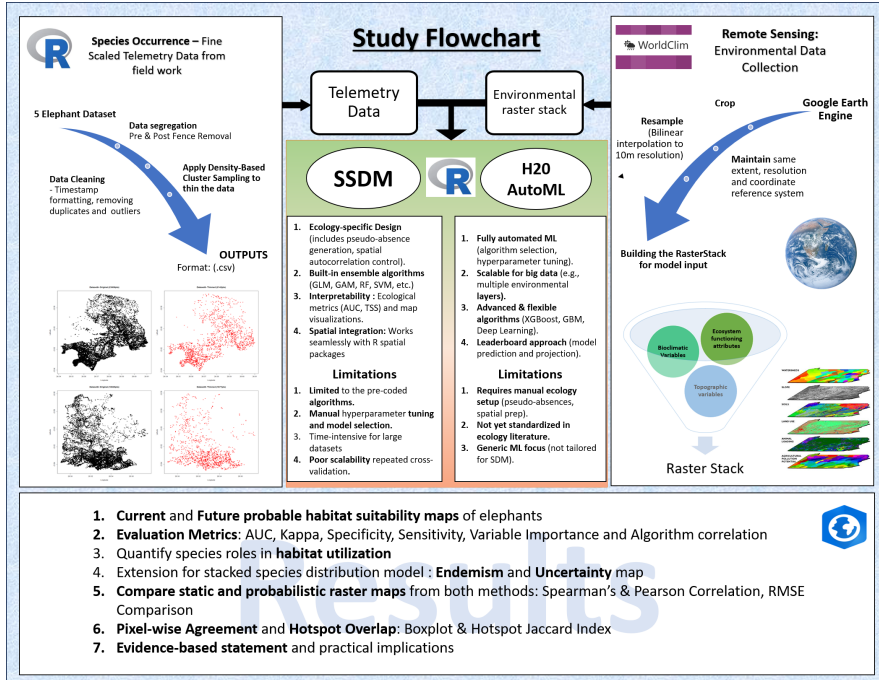
<sup>16</sup> **Abstract**

<sup>17</sup> Automated machine learning offers new opportunities to model  
<sup>18</sup> and predict the ecological trade-offs of fencing ecology for keystone  
<sup>19</sup> species. Fences however reveal reduction in human–wildlife conflict  
<sup>20</sup> and yet fragment habitats essentially undermining landscape connec-  
<sup>21</sup> tivity. This case study spatially analyzes the impact of fencing removal  
<sup>22</sup> on habitat suitability and utilization for 6 elephants in the Kariega  
<sup>23</sup> Game Reserve, South Africa. We utilized fine-scale telemetry data in  
<sup>24</sup> conjunction with high-resolution environmental co-variates to evaluate

two modeling methodologies: stacked ensemble species distribution models (SSDMs) and the h2o AutoML framework. To mitigate spatial autocorrelation, we implemented a density-based adaptive thinning algorithm (DBSCAN). Results show that the h2o AutoML approach efficiently outperformed SSDMs ( $AUC \approx 0.90$  vs.  $0.85$ ) in predictive accuracy, highlighting the potential to scale-up automated machine learning in spatial ecology. While both frameworks agreed and captured sharper, spatially explicit habitat gradients at broad scales (Pearson's  $r = 0.85\text{--}0.91$ ), AutoML revealed stronger post-fence expansion dynamics, underscoring how algorithmic flexibility shapes finer hotspot delineation. Pixel-wise difference maps based on Jaccard index effectively captured the telemetry movement patterns and fine-grained spatio-temporal change due to fence removal. We also found predicted range expansion from AutoML expanded by up to 35% while top 25% of both (AutoML vs SSDM) suitable pixels from the upper quartile ( $J_{0.75}$ ), quantified as core areas. Finally, the top-ranked h2o AutoML model, selected by cross-validated area under the Receiver Operating Characteristic Curve (AUC), was projected into various climate scenarios (Shared Socioeconomic Pathways (SSPs)) to evaluate shifts in future elephant habitat utilization. The findings not only highlight an interdisciplinary machine learning approach to inform landscape delineation for keystone species conservation, but addresses value for precise modeling strategies, contributing an open framework, and comprehensive benchmarking of AutoML frameworks complementing established

49 species distribution modeling pipelines.

## 50 Graphical Abstract



51

## 52 Highlights

- 53 • Automated Machine Learning improved accuracy and spatial detail of  
54 predictions compared to traditional SSDMs.
- 55 • Habitat expansion shifted markedly (by up to 35%) after fence removal  
56 for individual elephants.

- 57       • Between-framework differences reveal uncertainty critical for conserva-  
58              tion planning, emphasizing integration and greater efficiency.

59       **Keywords**

60       Species Distribution Model, H2O AutoML, Habitat utilization, Species-  
61              Environment interactions, Fence removal

62       **1     Introduction**

63       Landscape restoration for the conservation of keystone species and their  
64              habitat is crucial for preserving ecological stability, biodiversity, and resilience  
65              (Edwards et al. 2024) across various ecosystems. In an era of accelerating  
66              environmental change, their loss triggers cascading effects that fundamentally  
67              destabilize ecological networks and compromise essential ecosystem services  
68              (Ratajczak et al. 2022; Naidoo et al. 2025; Tobias et al. 2025). Many keystone  
69              species are becoming highly vulnerable to climate change, land-use change,  
70              and increasing human pressures (Edwards et al. 2024; Kau et al. 2025).  
71       Out of the many management interventions, fence removal stands central  
72              to the continuing debate on land sharing vs land sparing in human-wildlife  
73              coexistence (Grass et al. 2019). The most direct management challenge  
74              in southern Africa is wildlife fencing, established mainly to keep wildlife  
75              within reserves while boosting eco-tourism. Although boundary fences can

<sup>76</sup> substantially reduce human-wildlife conflict, internal fences may disrupt key  
<sup>77</sup> ecological connectivity for wide-ranging animals like elephants (Kremen 2015;  
<sup>78</sup> Osipova et al. 2018; Schwandner et al. 2025; Naidoo et al. 2025).

<sup>79</sup> Particularly, keystone megafauna such as African elephants epitomize the  
<sup>80</sup> tension between conservation and landscape modification for human well-being  
<sup>81</sup> (Van de Water et al. 2024; Gross 2024). Elephants serve as ecosystem engineers,  
<sup>82</sup> influencing biodiversity and ecological processes via seed dissemination, canopy  
<sup>83</sup> alteration, soil and water management, and creating micro habitats (Kau  
<sup>84</sup> et al. 2025; Timóteo et al. 2022). Yet these functions are threatened by  
<sup>85</sup> poaching, habitat fragmentation, and climate change (Nampindo and Randhir  
<sup>86</sup> 2024). Over the past fifty years, savanna elephant numbers have dropped by  
<sup>87</sup> around 70%, while forest elephant populations decreased by 90%, leading to an  
<sup>88</sup> estimated continental reduction of 77% (Edwards et al. 2024). Simultaneously,  
<sup>89</sup> atmospheric CO<sub>2</sub> concentrations have risen to 420 ppm, amplifying climate  
<sup>90</sup> extremes and compounding pressures on keystone taxa habitat (Hönisch et al.  
<sup>91</sup> 2023; Riva et al. 2024). These elements make elephants not only a conservation  
<sup>92</sup> priority but also a sensitive indicator species for assessing how landscape  
<sup>93</sup> modifications and management interventions affect ecosystem integrity.

<sup>94</sup> To quantify such changes, species distribution models (SDMs) provide  
<sup>95</sup> a key means of linking species' niche data with environmental variables,  
<sup>96</sup> providing spatial data for policymakers, reserve managers, and ecologists to  
<sup>97</sup> assess habitat suitability, predict spatial movements, and plan conservation  
<sup>98</sup> strategies (Elith and Leathwick 2009; Guisan and Zimmermann 2000). High-

99 resolution remote-sensing products, such as Sentinel-2 and MODIS, now supply  
100 continuous information on habitat data, vegetation, land cover, and human  
101 footprint. Leveraging them markedly improves SDM predictive performance  
102 (Agrillo et al. 2021; Jochems et al. 2024; Estopinan et al. 2022; Choe, Chi,  
103 and Thorne 2021; Kumari and Karthikeyan 2023). Integrating fine-scaled  
104 species occurrence data with machine learning yields geographically refined  
105 forecasts that inform proactive conservation and connectivity strategies (Tuia  
106 et al. 2022).

107 Traditionally, SDMs utilize techniques such as maximum entropy (Max-  
108 Ent), random forests, generalized linear models (GLMs), generalized additive  
109 models (GAMs), and support vector machines (SVMs). Despite their efficacy,  
110 these algorithms require substantial model calibration, parameter tuning, in-  
111 creased computational demand, and are often prone to collinearity, sampling  
112 bias, and overfitting (De Marco and Nóbrega 2018; Dormann et al. 2012;  
113 Phillips and Dudík 2008; Syphard and Franklin 2009; Valavi et al. 2018).  
114 Ensemble approaches, like those in the SSDM package, address underlying  
115 problems by integrating multiple algorithms (Kindt 2018; Schmitt et al. 2017).  
116 Yet ensemble SDMs remain difficult to scale and standardize, limiting repro-  
117 ducibility in applied contexts. Several studies (**Smith2022**; Feng et al. 2019;  
118 Gilman and Chaloupka 2024; Hesselbarth et al. 2024) highlight the absence of  
119 systematic benchmarking or reporting standards, making model comparison  
120 and scalability challenging. Automated machine learning (AutoML) offers  
121 a scalable alternative. By automating algorithm selection, hyperparameter

optimization, and ensemble integration, AutoML frameworks enhance reproducibility and reduce user bias while maintaining predictive power (Conrad et al. 2022; Feurer, Eggensperger, et al. 2020). Early applications in engineering (Omar et al. 2023; Tian and Che 2024) indicate AutoML can streamline ecological modeling (Gaber et al. 2024), but systematic benchmarks against established ensemble SDMs are scarce, especially for species-specific conservation problems (Zurell et al. 2020; Kass et al. 2024). We hypothesize that AutoML offers a more encouraging outlook with stronger gains and lasting impact, while SSDM provides a more cautious, stability-focused perspective. Given persistent challenges in SDM reproducibility and the absence of standardized reporting protocols (Zurell et al. 2020; Feng et al. 2019), open-access code and transparent workflows are essential for enabling independent verification, methodological refinement, and collaborative advancement in conservation science (Hesselbarth et al. 2024; Kass et al. 2024). Addressing this gap is critical for assessing the credibility of AutoML-derived outputs and underscores methodological integrity in forecasting dynamic ecological futures.

Relatively few studies have combined fine-scale telemetry with high-resolution environmental predictors for elephants, despite the potential of such integration (Fieberg et al. 2021; Giliba et al. 2023; Hebblewhite and Haydon 2010). Telemetry data reveals movement and habitat use at the level of individual decisions, while remote sensing provides continuous landscape gradients. Together, AutoML enables fine-grained SDMs that link species

145 behavior directly to dynamic environmental conditions. In this study, we  
146 benchmark h2o AutoML (H2O.ai 2024) against traditional ensemble SDMs  
147 using elephant telemetry data from Kariega Game Reserve, South Africa.  
148 Specifically, we evaluate differences in predictive accuracy, computational  
149 efficiency, and spatial predictions, while examining how targeted fence removal  
150 influences habitat suitability and potential range expansion, thereby informing  
151 connectivity restoration strategies for elephant populations in fragmented  
152 landscapes (Friswold et al. 2023; Naha et al. 2023). Through this approach, we  
153 propose a reproducible, scalable machine-learning framework that enhances  
154 predictive modeling for keystone species and provides actionable insight for  
155 conservation planning.

## 156 **2 Methodology**

### 157 **2.1 Data Collection and Pre-processing**

### 158 **2.2 Study Area**

159 The Kariega Game Reserve, located in the Eastern Cape province of South  
160 Africa, is a premier private wildlife conservancy spanning approximately  
161 10,000 hectares ( $115 \text{ km}^2$ ) along the Bushmans River. The reserve lies  
162 9.5 km inland from the Indian Ocean and is dominated by dense, woody, and  
163 thorny semi-succulent vegetation characteristic of the Albany Thicket biome.  
164 Kariega supports a diverse assemblage of wildlife, including African elephant

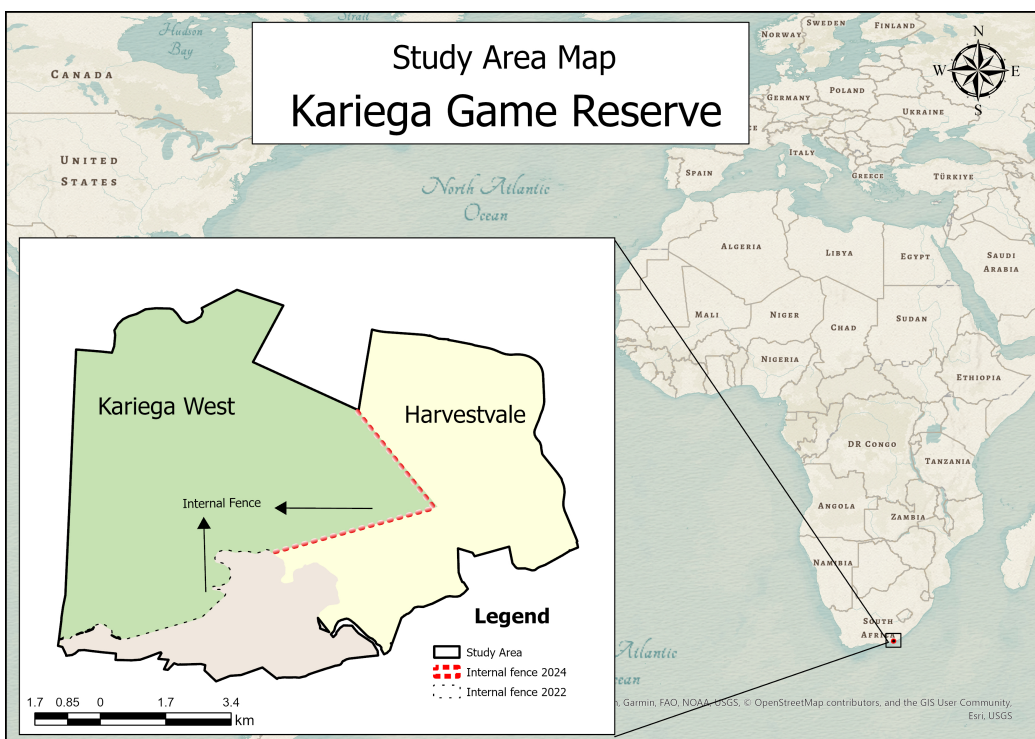


Figure 1: Study Area Map.

<sup>165</sup> (*Loxodonta africana*), giraffe (*Giraffa camelopardalis*), cheetah (*Acinonyx jubatus*), white and black rhinoceros (*Ceratotherium simum* and *Diceros bicornis*), ostrich (*Struthio camelus*), and numerous avian and reptile species.

<sup>168</sup> At the start of this study, the elephant population (75 individuals) was  
<sup>169</sup> divided by an internal fence into two sectors: Kariega West (KW; 2,792 ha;  
<sup>170</sup> 55 elephants) and Harvestvale (HV; 4,369 ha; 20 elephants). Fence removal  
<sup>171</sup> at Kariega occurred in two phases: in September 2022, HV was expanded  
<sup>172</sup> by 1,031 ha following the first internal fence removal. A second removal in  
<sup>173</sup> January 2024 eliminated the primary barrier between KW and HV, creating  
<sup>174</sup> a contiguous 8,192 ha landscape accessible to the entire elephant population  
(Friswold et al. 2023) (fig 1). To monitor spatial responses to habitat expansion,

Table 1: Dataset summary showing elephant IDs, record counts, temporal coverage before and after fence removal, and the number of points retained after DBSCAN spatial thinning.

Dataset	ID	Count	Earliest	Latest	DBSCAN
<b>Before Jan 2024</b>					
E1B	Kamva	12,364	09-01-2022 00:07	04-12-2023 23:40	1,106
E2B	Kambaku	10,364	09-01-2022 00:03	02-12-2023 23:40	927
E3B	Bukela	23,816	09-01-2022 00:07	31-12-2023 23:44	2,128
E4B	Half Moon	23,808	09-01-2022 00:23	31-12-2023 23:50	2,133
E5B	Beauty	18,629	09-01-2022 00:09	31-12-2023 23:56	1,671
E6B	Balu	21,259	09-02-2022 09:44	29-11-2023 17:45	1,901
<b>After Jan 2024</b>					
E3A	Bukela	25,091	01-01-2024 01:14	02-12-2025 23:54	2,246
E4A	Half Moon	24,999	01-01-2024 01:21	02-12-2025 23:56	2,244
E5A	Beauty	1,846	01-01-2024 01:57	14-02-2025 23:56	166
<b>Total</b>	–	<b>162,175</b>	–	–	<b>14,522</b>

<sup>175</sup>

<sup>176</sup> six African elephants (three solitary adult bulls and three matriarchs) were

<sup>177</sup> fitted with XL LoRa GPS collars (African Wildlife Tracking) in August 2022.  
<sup>178</sup> Collars recorded locations every 30 minutes, enabling detailed analysis of daily  
<sup>179</sup> movement patterns before and after fence removal. Data were transmitted  
<sup>180</sup> remotely through the LoRa system and managed via EarthRanger software  
<sup>181</sup> (Vulcan Inc. 2025).

<sup>182</sup> The telemetry dataset was subsequently cleaned and quality controlled.  
<sup>183</sup> Duplicate timestamps and erroneous points were removed, and records were  
<sup>184</sup> standardized across individuals. The conclusive dataset encompassed a three-  
<sup>185</sup> year duration, consisting of 127,717 GPS coordinates. Five datasets docu-  
<sup>186</sup> mented elephants before fence removal (09-01-2022 to 31-12-2023), whereas  
<sup>187</sup> three monitored matriarchs after fence removal (01-01-2024 to 02-12-2025)  
<sup>188</sup> (Table 1). Two matriarchs (E3 and E4) originated from the Kariega West  
<sup>189</sup> (KW) section (55 elephants), while matriarch E5 was from the Harvesvale  
<sup>190</sup> (HV) section (20 elephants). The GPS collar on E5 ("Beauty") experienced  
<sup>191</sup> device malfunction four months post-fence removal, yielding a smaller dataset  
<sup>192</sup> ( $n = 1,121$  points) but still spanning a full year. Despite this, each file  
<sup>193</sup> contained sufficient records for robust habitat utilization maps and temporal  
<sup>194</sup> species distribution models (SDMs).

### <sup>195</sup> 2.3 Data Thinning

<sup>196</sup> Considering the 10m resolution of environmental covariates, we applied spatial  
<sup>197</sup> thinning to avoid autocorrelation of GPS fixes. We used the Density-Based  
<sup>198</sup> Spatial Clustering of Applications with Noise (DBSCAN) algorithm (Hahsler,

199 Piekenbrock, and Doran 2019), a clustering method well suited for ecological  
200 applications that identifies clusters of arbitrary shape while distinguishing  
201 noise (Fuchs and Höpken 2022). Unlike  $k$ -means clustering, DBSCAN de-  
202 fines clusters based on point density, making it effective for irregular spatial  
203 distributions of animal movement data.

204 Retaining local density is crucial for SDM predictive accuracy, as it  
205 preserves the spatial structure of occurrence data relative to environmental  
206 covariates. Individual telemetry data includes transient movements that  
207 may overestimate suitable habitat (Schurr et al. 2012; Frantz et al. 2024).  
208 Inflated spatial autocorrelation, biased estimates, and reduced computational  
209 efficiency are common when unthinned GPS data is used, especially when  
210 environmental predictors are available at coarser resolutions than movement  
211 data. This was particularly relevant for our high-frequency dataset (30-minute  
212 intervals) with occasional irregularities due to network coverage gaps.

213 We implemented DBSCAN using the `dbscan` package in R with four pa-  
214 rameters: (i) neighbourhood radius (`eps_value` = 0.004 degrees,  $\sim$ 400 m); (ii)  
215 minimum points per cluster (`minPts_value` = 10); (iii) fraction retained per  
216 cluster (`fraction_value` = 0.2); and (iv) minimum samples for small clusters  
217 (`min_samples_value` = 4). This strategy balanced down-sampling while  
218 retaining spatial heterogeneity and density patterns. Thinning was applied  
219 separately to each individual (E1B, E2B, E3B, E4B, E5B, E3A, E4A, E5A,  
220 E6B), maintaining core spatial structure while eliminating redundant records  
221 and enhancing SDM robustness and computational efficiency (Figure 23).

222 **2.4 Environmental Data Preparation**

223 We assembled 26 environmental predictors from multiple high-resolution  
224 sources. NDVI and EVI were derived from Sentinel-2 imagery (10 m resolu-  
225 tion). Topographic variables (elevation, slope, aspect) were extracted from  
226 SRTM DEM (30 m). Aspect was converted to radians to produce cosine-  
227 aspect ("northness") for Southern Hemisphere orientation. Land cover was  
228 characterized using Global Forest Change and ESA WorldCover products  
229 (10–30 m). We incorporated 19 bioclimatic variables (BIO1–BIO19) from  
230 WorldClim at 1 km resolution, representing annual trends, seasonality, and  
231 extremes of temperature and precipitation (Choe, Chi, and Thorne 2021; Riva  
232 et al. 2024; Wang, Diao, and Lu 2024). To reduce multicollinearity, we eval-  
233 uated pairwise associations using Kendall's  $\tau$  correlation (Cohen 1960; Somers  
234 1962), excluding highly correlated predictors ( $r \geq 0.8$ ) via a correlation matrix  
235 19.

236 **2.5 Species Distribution Modeling Frameworks**

237 **2.5.1 Stacked Ensemble SDM (SSDM)**

238 The ensemble SDM workflow was implemented using the SSDM R pack-  
239 age (Schmitt et al. 2017). SSDM combines multiple algorithms including  
240 GLMs, GAMs, MARS, GBMs, CTAs, RFs, ANNs, and SVMs. Pseudoabsence  
241 points were generated internally to balance presence-only data, and mod-  
242 els were trained using holdout cross-validation (75% training, 25% testing).

243 Performance was evaluated with AUC, Cohen’s  $\kappa$  (Cohen 1960), sensitivity,  
244 and specificity (Fawcett 2006; Fleiss, Levin, and Paik 2003). By integrating  
245 multiple algorithms, SSDM ensembles reduce algorithm-specific biases and  
246 provide consensus predictions applicable to conservation planning (Naidoo  
247 et al. 2025; Guisan, Tingley, et al. 2013; Cheriyanda Raveendra, Picco, and  
248 Pirotti 2024).

249 **2.5.2 h2o AutoML Workflow**

250 We applied h2o AutoML using the `h2o` R package (Feurer, Eggensperger, et al.  
251 2020; Feurer and Hutter 2019). Equal pseudoabsence points ensured balanced  
252 training data. Environmental predictors were assembled into raster stacks,  
253 from which point-level values were extracted for each elephant dataset. Eight  
254 individual-specific models captured fine-scale habitat use variation. AutoML  
255 automatically trained base learners including GBMs, XGBoost, Deep Learning  
256 networks, DRF, and XRT, integrating them via a meta-learner weighted by  
257 cross-validated AUC (Feurer, Eggensperger, et al. 2020). Variable importance  
258 was aggregated across ensembles. Spatial predictions included: (i) current  
259 habitat suitability maps and (ii) future projections under four SSPs (SSP126,  
260 SSP245, SSP370, SSP585) for periods 2021–2040, 2041–2060, 2061–2080,  
261 and 2081–2100.

262 **2.6 Agreement Assessment Between Frameworks**

263 Following established protocols (Elith and Leathwick 2009; Kass et al. 2024;  
264 Konowalik and Nosol 2021; Maitner et al. 2025; Rausell-Moreno et al. 2025;  
265 Zurell et al. 2020), we evaluated internal consistency, spatial agreement, and  
266 temporal change mapping. Agreement between SSDM and h2o AutoML  
267 outputs was calculated using RMSE, Pearson’s  $r$ , and Spearman’s  $\rho$ . Jaccard  
268 index assessed core hotspot overlap for the top 25% of predicted suitability  
269 values. Raster differences and agreement maps visualized concordance and  
270 divergence between frameworks, exposing methodological biases and how  
271 modeling pipeline choice influences conservation inferences under dynamic  
272 conditions.

273 **2.7 Replicates and summary layers**

274 For each individual  $\times$  period  $\times$  method, three replicate models were fit.  
275 We derived per-pixel replicate summaries: mean  $\mu$ , standard deviation  $\sigma$ ,  
276 coefficient of variation  $CV = \sigma/(\mu + \varepsilon)$ , and stability  $\phi_t$  (fraction of replicates  
277 exceeding threshold  $t$ ). These diagnose internal consistency and inform map  
278 interpretation.

279 **2.8 Between-method agreement for all datasets**

280 To evaluate consistency between modeling pipelines, pixel-wise agreement was  
281 quantified using Pearson’s correlation coefficient ( $r$ ), Spearman’s rank corre-

282 lation ( $\rho$ ), root-mean-square error (RMSE), and mean absolute error (MAE).

283 :

284

$$r_{\text{Pearson}} = \frac{\sum_i (S_{\text{h2o}, i} - \bar{S}_{\text{h2o}})(S_{\text{SSDM}, i} - \bar{S}_{\text{SSDM}})}{\sqrt{\sum_i (S_{\text{h2o}, i} - \bar{S}_{\text{h2o}})^2} \sqrt{\sum_i (S_{\text{SSDM}, i} - \bar{S}_{\text{SSDM}})^2}}, \quad (1)$$

285

$$\text{RMSE} = \sqrt{\frac{1}{n} \sum_i (S_{\text{h2o}, i} - S_{\text{SSDM}, i})^2}, \quad (2)$$

286

$$\text{MAE} = \frac{1}{n} \sum_i |S_{\text{h2o}, i} - S_{\text{SSDM}, i}|. \quad (3)$$

287 Spatial difference maps ( $\Delta_{\text{method}} = S_{\text{h2o}} - S_{\text{SSDM}}$ ) were generated to  
288 visualize local divergence between modeling frameworks. Hotspot overlap  
289 was quantified using the Jaccard index (Real and Vargas 1996) on the upper-  
290 quartile masks (i.e., Intersection over Union).

291

$$J_{0.75} = \frac{\sum(H_{\text{h2o}} \wedge H_{\text{SSDM}})}{\sum(H_{\text{h2o}} \vee H_{\text{SSDM}})}, \quad H = [S > Q_{0.75}(S)], \quad (4)$$

292 This approach highlights how pipeline choice influences the delineation of  
293 priority cores, defined as the top 25% of suitability values. The upper-  
294 quartile threshold ( $Q_{0.75}$ ) isolates high-suitability “core” habitats for Jaccard  
295 comparison, minimizing noise from marginal regions. Additional thresholds  
296 ( $Q_{0.25}$ ,  $Q_{0.50}$ ,  $Q_{0.75}$ ) were applied to evaluate how model agreement and area  
297 change vary from broad potential range ( $Q_{0.25}$ ) to optimal core habitat ( $Q_{0.75}$ ).

298 **2.9 Temporal change analysis (E3, E4, E5)**

299 Following established transition matrix methodology (Pontius and Millones  
300 2011), temporal change was evaluated within each modeling framework for  
301 individuals with data spanning both periods (pre- and post-fence removal)

302 
$$\Delta_{A-B} = S_A - S_B, \quad (5)$$

303 where  $S_A$  denotes the habitat suitability map *after* fence removal, while  
304  $S_B$  represents the corresponding map *before* fence removal. The pixel-wise  
305 difference  $\Delta_{A-B} = S_A - S_B$  thus quantifies the direction and magnitude of  
306 temporal change in suitability. Positive values of  $\Delta_{A-B}$  indicate increased  
307 suitability following fence removal, negative values represent declines, and  
308 values near zero correspond to spatial stability. This continuous change  
309 surface captures both the intensity and spatial distribution of post-fence  
310 habitat shifts. Thereby using replicate means for each period, we computed  
311 the continuous difference and summarized categorical transitions at thresholds  
312  $t \in \{0.25, 0.50, 0.75\}$ . Let  $A_t = [S_A \geq t]$ ,  $B_t = [S_B \geq t]$ . We defined Gain,  
313 Stable and Loss classes as

314  $\text{Gain}_t = (A_t \wedge \neg B_t), \quad \text{Stable}_t = (A_t \wedge B_t), \quad \text{Loss}_t = (B_t \wedge \neg A_t), \quad (6)$

315 where  $\wedge$  denotes logical AND (intersection) and  $\neg$  denotes logical NOT  
316 (complement); thus, Gain, Stable, and Loss classes respectively represent

317 newly suitable, persistently suitable, and no-longer suitable habitats between  
318 periods (GSL maps). Then reported temporal overlap and area change as

319

$$J_t = \frac{\sum(A_t \wedge B_t)}{\sum(A_t \vee B_t)}, \quad \% \Delta \text{Area}_t = \frac{\sum A_t - \sum B_t}{\sum B_t + \varepsilon} \times 100. \quad (7)$$

320 Gain/Stable/Loss (GSL) maps,  $\Delta_{A-B}$  rasters, Jaccard-vs-threshold curves and  
321 % area-change summaries provide complementary, threshold-explicit views  
322 of post-fence responses. For each dataset we export base suitability maps  
323 for both methods, between-method difference maps, and CSV summaries of  
324 agreement metrics. For E3, E4 and E5 we additionally export  $\Delta_{A-B}$  rasters,  
325 GSL maps at the three thresholds, and temporal metrics tables. A panel  
326 composer assembles per-elephant dashboards (Before/After maps,  $\Delta$ , GSL  
327 strip, Jaccard values  $J_t$  and  $\% \Delta \text{Area}$ ) per elephant and method.

328 **2.10 Reproducibility**

329 All analyses were conducted in R (v4.3) using `terra`, `SSDM`, and `h2o`, with  
330 parallelisation on a multi-core workstation. Rasters were aligned via repro-  
331 jection, bilinear resampling for continuous layers and nearest-neighbour for  
332 binary outputs. Code paths, thresholds and file conventions are documented  
333 in the github repository (Aiyanna 2025) to ensure end-to-end reproducibility.

334 **3 Results**

335 **3.1 Model discrimination and between-method agree-**  
336 **ment**

Table 2: Between-method agreement metrics comparing h2o AutoML and SSDM predictions across all datasets.

Dataset	Pearson $r$	Spearman $\rho$	RMSE	MAE	Jaccard $_{0.75}$
E1B	0.952	0.926	0.096	0.058	0.787
E2B	0.928	0.910	0.115	0.066	0.772
E3B	0.947	0.911	0.110	0.066	0.789
E4B	0.946	0.922	0.112	0.069	0.796
E5B	0.936	0.917	0.102	0.068	0.680
E6B	0.929	0.916	0.108	0.072	0.684
E3A	0.878	0.886	0.113	0.088	0.597
E4A	0.839	0.840	0.170	0.133	0.577
E5A	0.856	0.861	0.206	0.143	0.597

337 Across eight telemetry datasets (E1B, E2B, E3B, E4B, E5B; E3A, E4A,  
338 E5A), we benchmarked h2o AutoML against stacked SDMs (SSDM). For  
339 elephants with before–after coverage (E3, E4, E5), temporal change was  
340 quantified as  $\Delta_{A-B} = S_A - S_B$ . Post-fence removal results indicated that  
341 reserve size and population density likely influenced habitat use, as two  
342 herds originated from the smaller, denser Kariega West (KW) section and  
343 one from the larger Harvestvale (HV) section. Results include continuous  
344 suitability surfaces, thresholded maps ( $Q_{0.25}$ ,  $Q_{0.50}$ ,  $Q_{0.75}$ ), and composite  
345 figures consolidating spatial predictions and summary metrics.

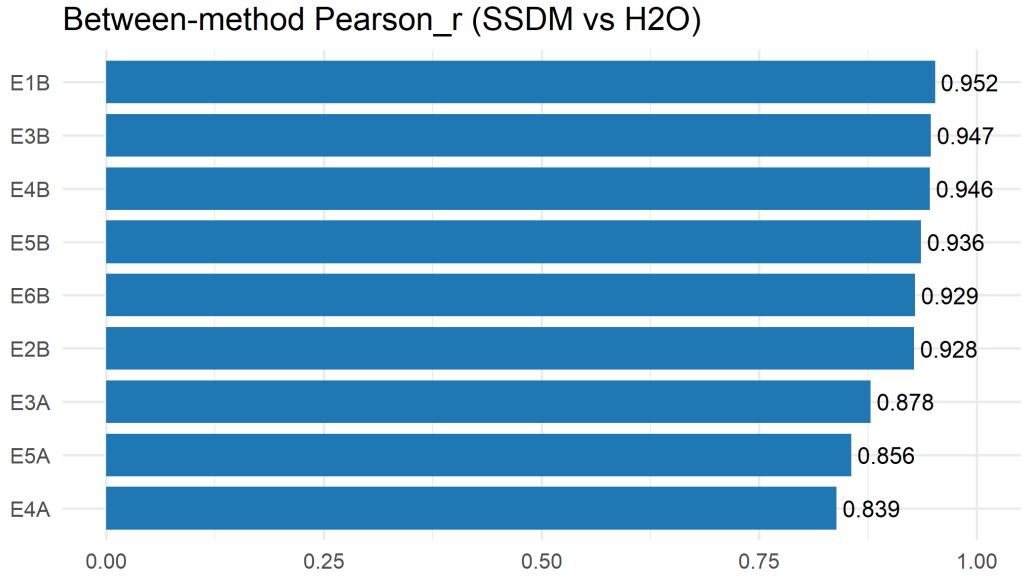


Figure 2: Pearson correlation between h2o AutoML and SSDM predictions across datasets.

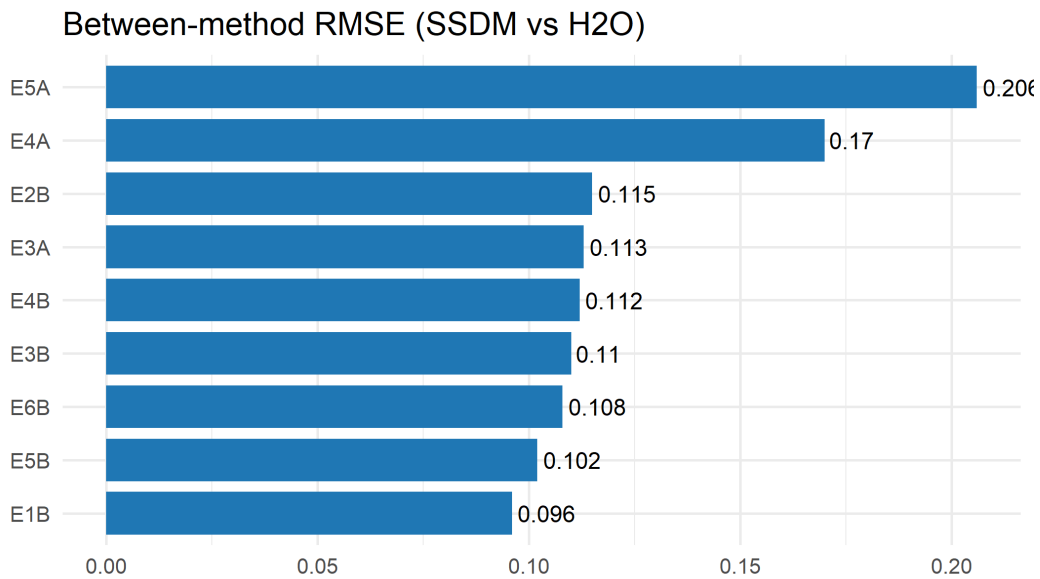


Figure 3: Root Mean Square Error (RMSE) comparing h2o AutoML and SSDM outputs.

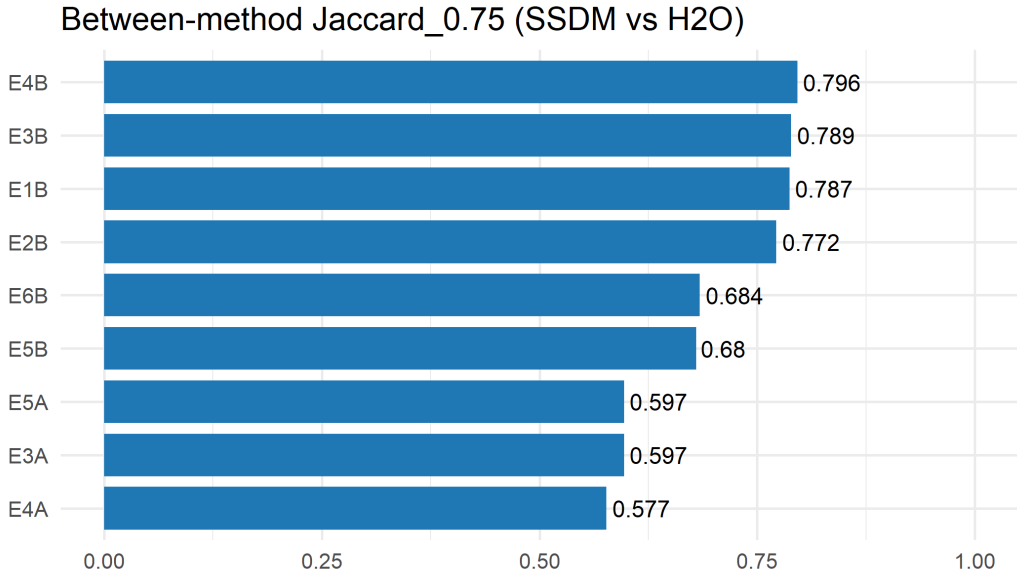


Figure 4: Hotspot Jaccard similarity (upper quartile, Q75) between h2o AutoML and SSDM predictions.

346 Both frameworks exhibited high correspondence in predicted suitability,  
 347 yet with systematic differences in magnitude and spatial detail (Table 2). Pixel-wise correlations were strong (Pearson’s  $r = 0.839\text{--}0.952$ ; Spearman’s  $\rho = 0.840\text{--}0.926$ ), indicating broad agreement in large-scale gradients.  
 349 However, local discrepancies remained non-negligible (RMSE 0.096–0.206;  
 350 MAE 0.058–0.143). Hotspot overlap, measured by Jaccard index on the  
 351 upper quartile ( $J_{0.75}$ ), was moderate (0.577–0.796), indicating substantial  
 352 core-habitat agreement despite high global correlations. Jaccard values showed  
 353 greater variability among matriarchs (0.684–0.787) than bulls, potentially  
 354 reflecting increased habitat heterogeneity following fence removal. Spatial  
 355 difference maps ( $S_{\text{h2o}} - S_{\text{SSDM}}$ ) revealed that most divergences occurred along  
 356

357 transitional zones and mixed-cover mosaics, where subtle environmental gra-  
358 dients amplify model-specific sensitivities.

359 **3.2 Environmental drivers of suitability**

360 Both frameworks converged on precipitation and temperature as primary  
361 drivers, particularly precipitation seasonality (BIO15), precipitation of the  
362 warmest quarter (BIO16), and maximum temperature of the warmest month (BIO5).  
363 Post-fence datasets exhibited increased importance of vegetation productivity  
364 indices (NDVI and EVI). Rank correlation of variable importance between  
365 frameworks exceeded 0.85 (Fig. 14), indicating strong consistency despite  
366 spatial divergence in predictions.

367 **3.3 Temporal change following fence removal (E3, E4 &  
368 E5)**

369 Both frameworks revealed strong threshold-dependent differences in habitat  
370 area and temporal change (Table 3), though with systematic framework di-  
371 vergence. At the permissive threshold ( $t = 0.25$ ), both predicted substantial  
372 habitat expansion following fence removal (SSDM: up to 51 km<sup>2</sup>; h2o: up to  
373 86 km<sup>2</sup>), indicating broad agreement on post-removal habitat gain. As thresh-  
374 olds became stricter ( $t = 0.50, 0.75$ ), suitable area decreased monotonically  
375 and framework divergence increased markedly. SSDM predicted substantial  
376 habitat loss for E3 ("Bukela", -50%) and E4 ("Half-Moon", 32.64%) at

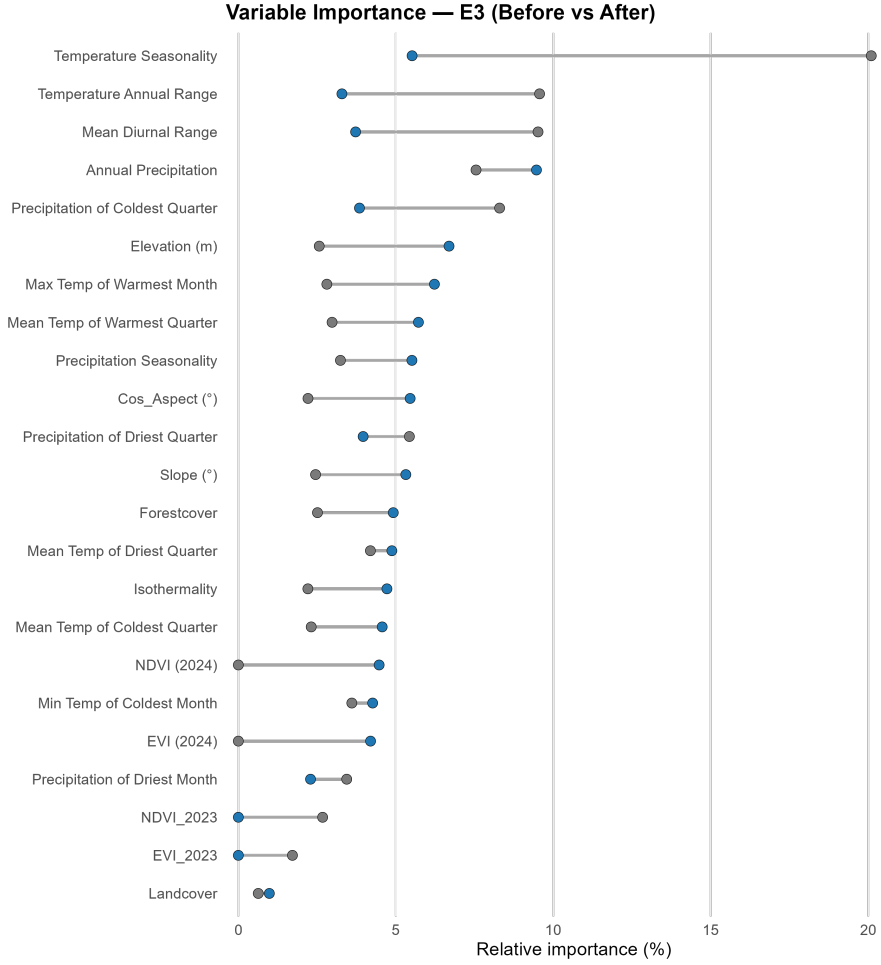


Figure 5: Elephant E3 (“Bukela”). Dumbbell plots display the relative contribution (%) of each environmental predictor to h2o AutoML and SSDM habitat suitability models in the pre-fence removal period (gray circles; before 2024) and post-fence removal period (blue circles; after 2024). Horizontal line spans indicate the magnitude of change in predictor importance between periods, with leftward shifts representing decreased importance and rightward shifts representing increased importance. The distance between circles illustrates how fence removal altered the relative weight of environmental drivers in explaining habitat-use patterns. Variable importance rankings remained strongly correlated (Spearman’s  $\rho > 0.85$ ) between frameworks, indicating agreement on dominant predictors despite differences in spatial detail. Figures for Elephant E4 (“Half-Moon”) and E5A (“Beauty”) are provided in the Appendix.

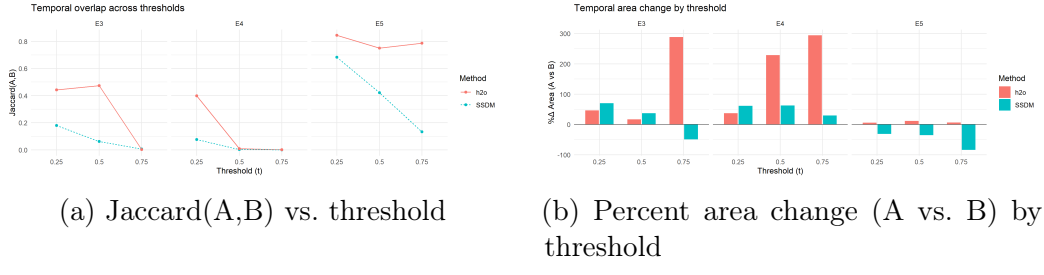


Figure 6: Temporal robustness: overlap and area change across thresholds (0.25, 0.50, 0.75) for E3, E4 and E5 within each framework.

Table 3: Temporal change metrics (Before–After) for elephants E3, E4, and E5 across three suitability thresholds ( $t \in \{0.25, 0.5, 0.75\}$ ) and two modelling frameworks (SSDM and h2o AutoML). Threshold  $t$  is the suitability cutoff.  $B_{\text{area}}$  and  $A_{\text{area}}$  are suitable habitat areas *Before* and *After* fence removal, respectively;  $\% \Delta \text{ Area} = \frac{A_{\text{area}} - B_{\text{area}}}{B_{\text{area}}} \times 100\%$ .  $J_t$  is the Jaccard similarity between Before and After maps (0–1). All areas are in  $\text{km}^2$ .

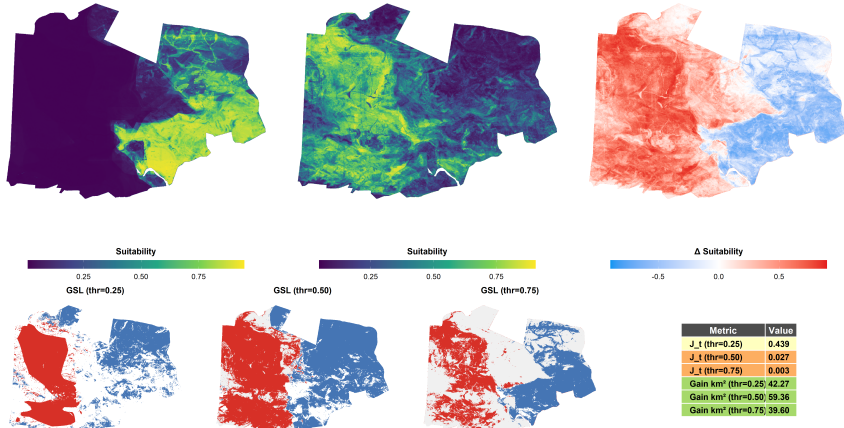
ID	Method	$t$	$B_{\text{area}}$ ( $\text{km}^2$ )	$A_{\text{area}}$ ( $\text{km}^2$ )	Loss ( $\text{km}^2$ )	Stable ( $\text{km}^2$ )	Gain ( $\text{km}^2$ )	$\% \Delta$ (%)	$J_t$
E3	SSDM	0.25	30.13	51.82	17.78	12.35	39.47	71.98	0.18
	SSDM	0.50	18.28	25.12	15.76	2.51	22.60	37.43	0.06
	SSDM	0.75	12.87	6.41	12.74	0.13	6.28	-50.18	0.01
	H <sub>2</sub> O	0.25	59.38	86.92	14.73	44.65	42.27	46.37	0.44
	H <sub>2</sub> O	0.50	18.36	61.44	16.28	2.08	59.36	234.59	0.03
	H <sub>2</sub> O	0.75	11.47	39.74	11.32	0.15	39.60	246.56	0.00
E4	SSDM	0.25	30.53	49.63	24.89	5.64	43.99	62.55	0.08
	SSDM	0.50	19.05	31.42	18.92	0.13	31.29	64.92	0.00
	SSDM	0.75	13.27	17.61	13.27	0.00	17.61	32.64	0.00
	H <sub>2</sub> O	0.25	59.80	80.07	19.97	39.84	40.24	33.90	0.40
	H <sub>2</sub> O	0.50	53.87	61.35	18.55	35.32	26.02	13.88	0.44
	H <sub>2</sub> O	0.75	10.87	42.83	10.76	0.11	42.72	294.16	0.00
E5	SSDM	0.25	35.35	24.40	11.11	24.25	0.15	-30.98	0.68
	SSDM	0.50	19.89	12.89	10.17	9.73	3.17	-35.19	0.42
	SSDM	0.75	8.53	1.40	7.36	1.17	0.23	-83.63	0.13
	H <sub>2</sub> O	0.25	67.67	70.76	4.34	63.34	7.42	4.56	0.84
	H <sub>2</sub> O	0.50	52.62	59.18	4.81	47.81	11.37	12.48	0.75
	H <sub>2</sub> O	0.75	42.88	45.64	3.85	39.03	6.62	6.45	0.79

377  $J_t = 0.75$ , with Jaccard indices of 0.01 indicating minimal temporal overlap of  
378 high-suitability cores. In contrast, h2o retained substantial core habitat at the  
379 strictest threshold (Jaccard up to 0.79 for E5A), indicating greater predicted  
380 persistence. For E5A ("Beauty"), frameworks diverged most sharply: SSDM  
381 predicted progressive contraction across all thresholds ( $-30\%$  to  $-83\%$ ),  
382 whereas h2o identified net persistence despite modest area reduction. These  
383 differences highlight how ensemble structures and algorithms influence tem-  
384 poral habitat projections. Jaccard similarity indices ( $J_t$ ) quantified spatial  
385 overlap between Before and After habitat maps at three thresholds ( $t = 0.25$ ,  
386 0.50, 0.75). h2o AutoML consistently showed higher temporal overlap than  
387 SSDM, particularly at moderate thresholds. For instance,  $J_{0.25}$  averaged  
388 0.44–0.84 for h2o but only 0.08–0.68 for SSDM, indicating more temporally  
389 coherent suitability patterns. At  $t = 0.75$ , overlap declined sharply for SSDM  
390 (often  $J_t = 0.01$ ), reflecting minimal persistence of high-suitability zones.  
391 In contrast, h2o exhibited moderate to high persistence (E3:  $J_{0.75} = 0.00$ ;  
392 E4:  $J_{0.75} = 0.002$ ; E5:  $J_{0.75} = 0.79$ ), with E5 showing notably stable core  
393 habitats ( $A = 42.88 \text{ km}^2$ ). Composite panels integrate base maps,  $\Delta$  maps,  
394 gain–stability–loss (GSL) strips, and metric tables (Figs 7, 12, 13).

### 395 3.4 Synthesis

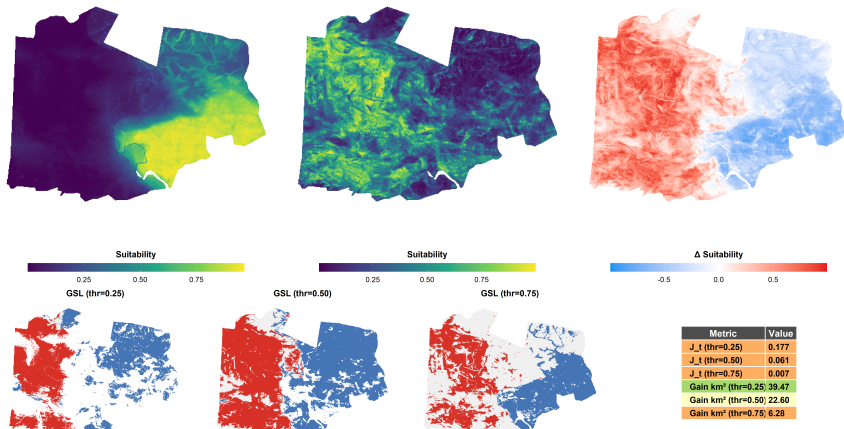
396 We observe three consistent patterns. (i) *Discrimination*: h2o AutoML  
397 outperformed SSDM across all datasets, achieving lower error and higher  
398 AUC. (ii) *Spatial agreement*: Global correlations were high, but hotspot

Elephant E3 — H<sub>2</sub>O | Before vs After: base maps,  $\Delta$  (A-B), GSL strip, temporal metrics



(a) E3 — H<sub>2</sub>O AutoML

Elephant E3 — SSDM | Before vs After: base maps,  $\Delta$  (A-B), GSL strip, temporal metrics



(b) E3 — SSDM

Figure 7: Per-elephant comparison for Bukela (E3). The upper panel shows habitat suitability maps before and after fence removal, with a difference map  $\Delta = A - B$  indicating increases (red) and decreases (blue) in suitability. The lower panel presents threshold-specific spatial changes: blue denotes areas that became suitable (Gain), red indicates areas that became unsuitable (Loss), and white shows areas that remained suitable (Stable) after the intervention. The accompanying table summarizes model metrics, Jaccard similarity (spatial overlap at each threshold) and percentage change in suitable area (% $\Delta$  area). All areas are in km<sup>2</sup>

overlap remained moderate and spatial difference maps revealed fine-scale divergence, particularly in transitional zones. (iii) *Temporal change*: Both frameworks detected post-fence habitat expansion, with h2o offering a more sensitive lens (sharper  $\Delta$ , larger gains) and SSDM providing a conservative baseline (smoother cores, higher stability). Together, these perspectives delineate the plausible uncertainty envelope for conservation interpretation and highlight the complementary insights of automated versus ensemble SDM approaches.

## 4 Discussion and Conservation implications

This study demonstrates that h2o AutoML consistently outperformed traditional SSDM across multiple performance metrics. AutoML achieved superior discrimination (higher ROC–AUC), calibration (lower RMSE and log-loss), and computational efficiency, revealing stronger capacity to capture nonlinear environmental responses (Feurer and Hutter 2019; H2O.ai 2024). Unlike traditional ensemble approaches (Schmitt et al. 2017) using fixed weighting, AutoML adaptively reweighted base learners to match each elephant’s movement data structure. GBM- and XRT-dominated ensembles captured Bukela’s patterns, while Half-Moon required deeper neural networks, and Beauty’s smaller sample was represented by simpler GBM architecture. AutoML’s robustness maintained high predictive accuracy (Gilman and Chaloupka 2024), adding rigor to future climatic extrapolations. These findings align

420 with evidence that machine learning automation enhances predictive power in  
421 wildlife conservation (Tuia et al. 2022; Gaber et al. 2024), while its parallelized  
422 architecture (Conrad et al. 2022) substantially reduced training time.

423 Addressing collinearity is fundamental for reliable inference (De Marco  
424 and Nóbrega 2018; Dormann et al. 2012). While VIF and PCA are widely  
425 used, both have drawbacks: VIF is sensitive to sample size; PCA obscures  
426 ecological meaning (Dormann et al. 2012). This study employed Kendall’s  $\tau$   
427 rank correlation for variable screening (Feng et al. 2019), preserving biological  
428 interpretability while maintaining predictive performance. Spatial block  
429 cross-validation (Roberts et al. 2017; Valavi et al. 2018) confirmed predictive  
430 stability across spatially independent partitions (Figs. 16, 18). By pre-  
431 screening variables for ecological interpretability, AutoML focused automated  
432 feature selection on biologically meaningful predictors (Feurer and Hutter  
433 2019; Tuia et al. 2022), balancing accuracy with transparency—critical for  
434 conservation decision-making (Gilman and Chaloupka 2024).

435 Pre- and post-fence outputs (Table 3) provide compelling evidence of  
436 restoring landscape connectivity value. Before removal, elephants occupied  
437 restricted, fragmented habitats; post-removal revealed clear expansions into  
438 newly accessible terrain, mirroring broader evidence that fences constrain  
439 movement and erode long-term viability (Kau et al. 2025; Naha et al. 2023).  
440 Site-specific differences in reserve configuration shaped initial habitat use,  
441 with localized population densities (KW: 55 elephants; HV: 20 elephants) and  
442 spatial heterogeneity mediating connectivity gains (Schwandner et al. 2025).

443        Individual responses revealed significant habitat expansion (??). Matri-  
444        arch Bukela (E3A) demonstrated the most pronounced expansion (Fig. 7),  
445        suggesting experienced individuals effectively identify and utilize restored  
446        connectivity. AutoML maintained stronger temporal consistency for Bukela,  
447        preserving continuous high-suitability patches under strict thresholds, while  
448        SSDM fragmented predicted areas. Half-Moon (E4) displayed heterogeneous  
449        patterns with sharp gain-loss mosaics, reflecting exploratory use typical of  
450        post-barrier investigations (Osipova et al. 2018; Naha et al. 2023). Beauty (E5)  
451        showed modest but coherent expansion along existing corridors, retaining sta-  
452        ble cores—suggesting her herd had established optimal habitat selection with  
453        expansion following established movement patterns (Wall et al. 2014; Bohrer  
454        et al. 2014). Expansion for both Bukela and Half-Moon was directed toward  
455        Harvestvale, indicating restored connectivity enabled access to previously  
456        inaccessible high-quality patches. These patterns highlight the importance  
457        of assessing habitat change across multiple thresholds to identify expansion  
458        fronts and persistent refugia (Roberts et al. 2017; Valavi et al. 2018).

459        Despite AutoML’s superior accuracy, it exhibited limited spatial congru-  
460        ence with SSDM, sharing only 17–28% of high-suitability areas, consistent  
461        with benchmarking studies showing algorithmic ensembles often differ spa-  
462        tially despite comparable discrimination scores (Fischer and Lindenmayer  
463        2007; Grass et al. 2019). Difference maps ( $\Delta = S_{\text{AutoML}} - S_{\text{SSDM}}$ ) reveal  
464        h2o AutoML precisely delineated fence boundaries with sharp transitions  
465        corresponding to physical barrier locations, while SSDM provided moderate

<sup>466</sup> spatial separation. This highlights AutoML's enhanced sensitivity to complex  
<sup>467</sup> ecological discontinuities and ability to capture fine-scale habitat boundaries  
<sup>468</sup> critical for conservation planning. Cross-framework comparisons expose pre-  
<sup>469</sup> dictive confidence boundaries, underscoring the value of ensemble approaches  
<sup>470</sup> incorporating multiple algorithmic perspectives for high-stakes conservation  
<sup>471</sup> decisions (**Arajo2007**; Schmitt et al. 2017).

<sup>472</sup> Precipitation and temperature variables (Figs. 14, 14a, 14b) emerged as  
<sup>473</sup> dominant predictors, consistent with water-dependent megafauna ecology  
<sup>474</sup> requiring reliable surface water and thermally suitable foraging areas (Loarie,  
<sup>475</sup> Aarde, and Pimm 2009; Bohrer et al. 2014). Following fence removal, vege-  
<sup>476</sup> tation indices (NDVI, EVI) gained prominence, indicating elephants rapidly  
<sup>477</sup> exploited newly accessible, high-productivity areas, suggesting quality forage  
<sup>478</sup> became more influential once barriers were removed (Wall et al. 2014).

<sup>479</sup> Forward projections revealed contrasting trajectories through 2100. Under  
<sup>480</sup> low-emission scenarios (SSP1–2.6), suitable habitat remained stable, suggest-  
<sup>481</sup> ing current conservation areas may continue supporting populations. However,  
<sup>482</sup> high-emission pathways (SSP5–8.5) predicted substantial habitat loss, consis-  
<sup>483</sup> tent with projected climate refugia contractions (Naidoo et al. 2025; Pacifici  
<sup>484</sup> et al. 2017). These projections emphasize the critical importance of maintain-  
<sup>485</sup> ing and expanding connectivity now, as gains achieved through fence removal  
<sup>486</sup> may prove essential for enabling climate-driven range shifts.

<sup>487</sup> Several limitations constrain broader generalization. After initial fence  
<sup>488</sup> removal, collared bulls concentrated within Harvestvale while E6B explored

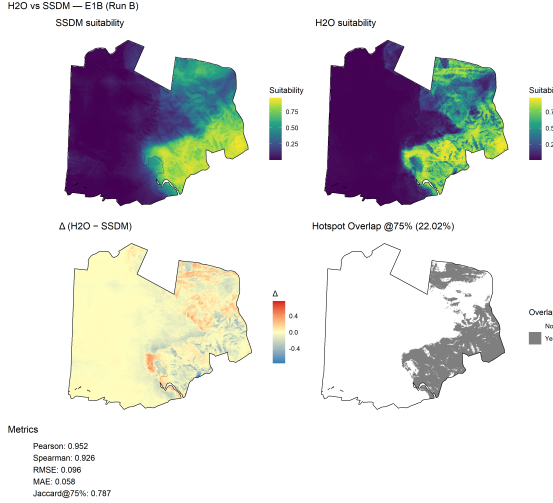


Figure 8: Pre-fence removal habitat suitability map for male elephant E1B (“Kambaku”).

widely (Fig. 8–10), and suitability maps revealed persistent patterns along remaining internal fences, indicating incomplete connectivity restoration. Only complete fence removal enabled substantial habitat expansions, suggesting incremental improvements may be insufficient. Individual-level variation—Bukela’s extensive utilization versus Beauty’s corridor-following—suggests conservation strategies must account for behavioral diversity. All three bulls experienced collar twisting within six months, necessitating removal and losing male movement data post-2024( Friswold et al. 2023). Small sample size (six elephants, reduced to three post-fence) restricts understanding of gender-specific responses. Correlative models cannot fully capture behavioral or physiological processes underlying habitat selection( Boyce et al.

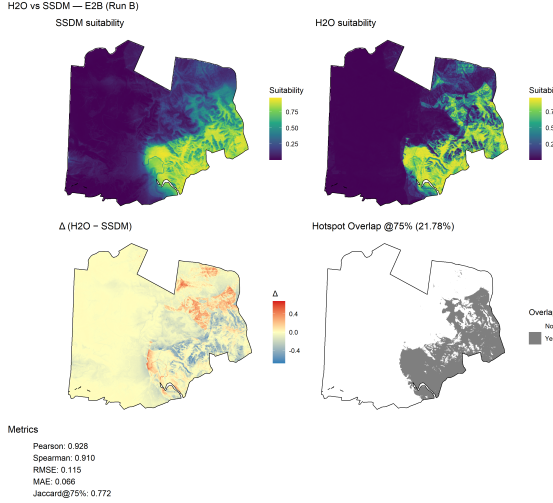


Figure 9: Pre-fence removal habitat suitability map for male elephant E2B (“Kamva”).

500 2002; Matthiopoulos et al. 2015), and short-term disturbances (droughts,  
 501 fires, anthropogenic pressures) remain inadequately represented with only  
 502 abiotic predictors. Future research should integrate mechanistic approaches  
 503 (RSFs, SSFs) with AutoML frameworks to capture biological realism (Boyce  
 504 et al. 2002; Fieberg et al. 2021; Hebblewhite and Haydon 2010). Dynamic  
 505 connectivity models (Gilman and Chaloupka 2024; Wilkinson et al. 2025)  
 506 and energetically informed dispersal kernels (Sullivan et al. 2018) could  
 507 provide realistic representations of movement costs. Incorporating multi-  
 508 modal datasets (Stasinou et al. 2025)—remote sensing time series, acoustic  
 509 monitoring, genetic sampling, human–wildlife conflict data—could enable  
 510 comprehensive predictions (Tuia et al. 2022; Guisan, Tingley, et al. 2013;

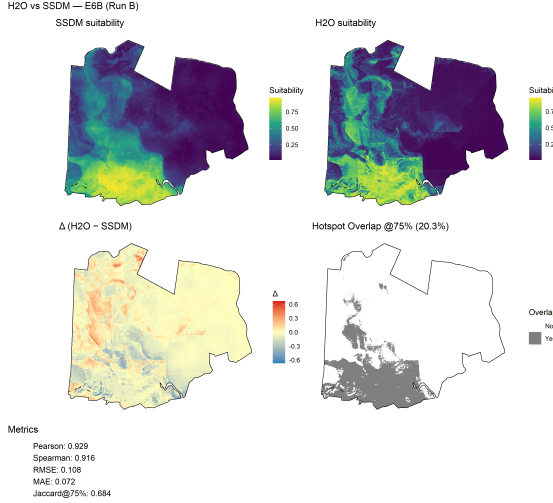


Figure 10: Pre-fence removal habitat suitability map for male elephant E6B (“Balu”).

511 Karp et al. 2025). AutoML’s computational efficiency suggests significant  
 512 potential for scaling to landscape, regional, or continental analyses. Embrac-  
 513 ing open science principles through open-source code sharing, benchmarked  
 514 validation protocols, and transparent reporting (Zurell et al. 2020; Hesselbarth  
 515 et al. 2024) is critical to advancement. Practical conservation implications  
 516 are immediate and urgent. Quantified habitat gains following fence removal  
 517 (Table 3) provide strong empirical support for connectivity restoration. Our  
 518 open-sourced code (Aiyanna 2025) leverages AutoML’s precise delineation of  
 519 expansion areas to inform targeted protection efforts, anti-poaching patrol  
 520 routes, and human–wildlife conflict mitigation in newly utilized habitats.  
 521 Climate projections (Fig. 11) indicating substantial habitat loss under high-

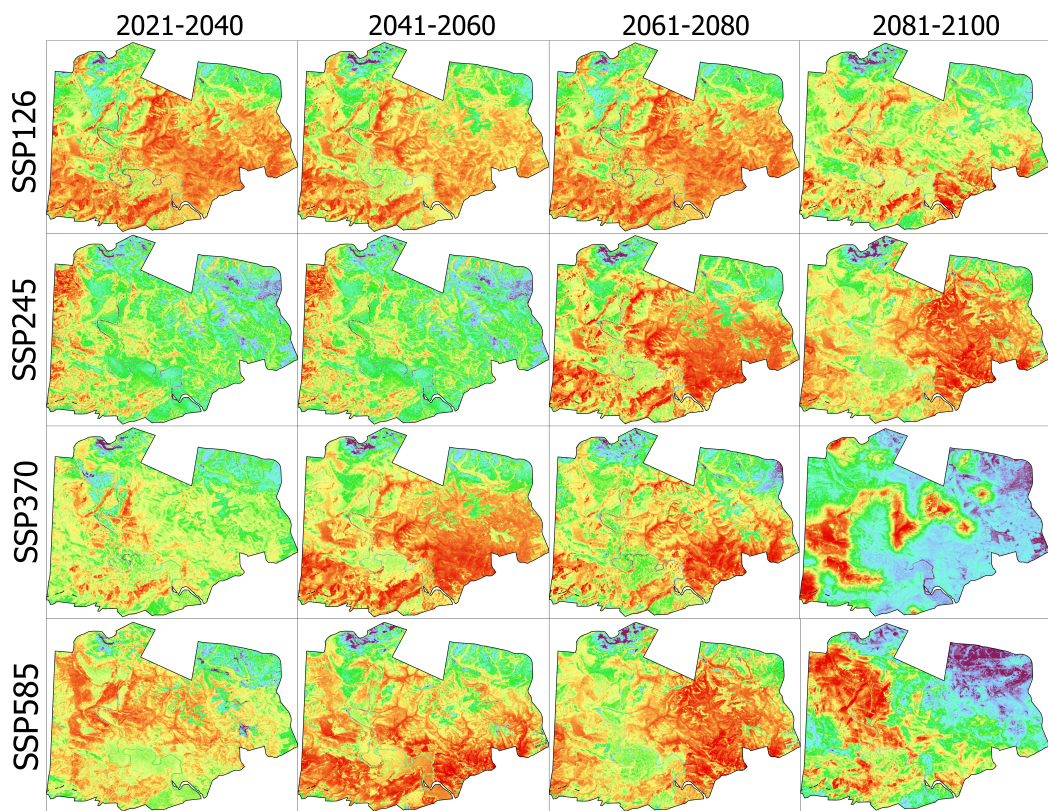


Figure 11: Future projection for Bukela-E3A.

522 emission scenarios emphasize urgency of current connectivity restoration  
523 efforts (Naidoo et al. 2025; Pacifici et al. 2017). Spatial divergence between  
524 AutoML and SSDM highlights the importance of using multiple approaches  
525 for high-stakes conservation decisions, with management plans incorporating  
526 uncertainty estimates across modeling approaches. By combining AutoML’s  
527 scalability with mechanistic ecological understanding and multimodal data  
528 integration, future research can advance toward adaptive, data-rich conser-  
529 vation strategies reflecting ecological complexity and practical management  
530 constraints while maintaining transparency and reproducibility essential for  
531 science-based conservation policy.

## 532 5 Conclusion

533 This study demonstrates that AutoML represents a significant advancement  
534 in habitat suitability modeling for conservation applications, offering superior  
535 predictive performance, computational efficiency, and replicability compared  
536 to traditional ensemble approaches. The framework’s ability to adaptively  
537 optimize model architecture while being ecologically interpretable makes it  
538 particularly valuable for species-specific conservation planning. The quantified  
539 benefits of fence removal provide compelling evidence for landscape connectiv-  
540 ity restoration as an effective conservation strategy, with individual elephants  
541 rapidly exploiting newly accessible, high-quality habitats. However, the spatial  
542 divergence between modeling frameworks and the projected impacts of climate

543 change underscore the importance of adaptive management approaches that  
544 decomposes multiple sources of uncertainty. Crucially analyzing stochastic or  
545 data-driven (telemetry and thinning), algorithmic (AutoML vs. SSDM) and  
546 temporal (prediction stability) uncertainty, SDMs form an integral component  
547 to strengthen large-scale landscape restoration policies. Looking forward, the  
548 integration of AutoML with mechanistic models, multimodal datasets, and  
549 open-source frameworks offers a pathway toward more robust, scalable, and  
550 policy-relevant conservation tools. As automated machine learning capabili-  
551 ties continue to evolve, their application to conservation challenges promises  
552 to enhance our ability to protect biodiversity in an increasingly complex  
553 and rapidly changing world. The success of fence removal in this system  
554 provides a template for similar connectivity restoration efforts globally, while  
555 the methodological advances demonstrated here offer tools for more effective  
556 conservation planning across species and ecosystems. Most importantly, this  
557 work illustrates how cutting-edge computational approaches can be harnessed  
558 to address urgent conservation challenges, providing both immediate manage-  
559 ment guidance and a foundation for adaptive, evidence-based conservation  
560 strategies.

## 561 References

562 Agrillo, Emiliano, Federico Filippini, Alice Pezzarossa, Laura Casella, Daniela  
563 Smiraglia, Arianna Orasi, Fabio Attorre, and Andrea Taramelli (Mar.

- 564        2021). “Earth Observation and Biodiversity Big Data for Forest Habitat  
565        Types Classification and Mapping”. In: *Remote Sensing* 13.7, p. 1231.  
566        ISSN: 2072-4292. DOI: 10.3390/rs13071231. URL: <http://dx.doi.org/10.3390/RS13071231>.
- 568        Aiyanna, Harin (2025). *MySpeciesSDM: R code for species distribution mod-*  
569        *eling with H2O AutoML*. R scripts. Accessed: 2025-10-28. URL: [https://github.com/Caspian-Aiyanna/ems\\_paper.git](https://github.com/Caspian-Aiyanna/ems_paper.git).
- 571        Bohrer, Gil, Pieter SA Beck, Shadrack M Ngene, Andrew K Skidmore, and  
572        Ian Douglas-Hamilton (Jan. 2014). “Elephant movement closely tracks  
573        precipitation-driven vegetation dynamics in a Kenyan forest-savanna land-  
574        scape”. In: *Movement Ecology* 2.1. ISSN: 2051-3933. DOI: 10.1186/2051-  
575        3933-2-2. URL: <http://dx.doi.org/10.1186/2051-3933-2-2>.
- 576        Boyce, Mark S, Pierre R Vernier, Scott E Nielsen, and Fiona K.A Schmiegelow  
577        (Nov. 2002). “Evaluating resource selection functions”. In: *Ecological Mod-*  
578        *elling* 157.2–3, pp. 281–300. ISSN: 0304-3800. DOI: 10.1016/s0304-  
579        3800(02)00200-4. URL: [http://dx.doi.org/10.1016/S0304-3800\(02\)00200-4](http://dx.doi.org/10.1016/S0304-3800(02)00200-4).
- 581        Cheriyanda Raveendra, Harin Aiyanna, Lorenzo Picco, and Francesco Pirotti  
582        (Nov. 2024). “Using Earth observation to support the predictive accuracy of  
583        species distribution models in ecological restoration: a case study of Poland  
584        beavers (*Castor fiber*)”. In: *The International Archives of the Photogrammetry,*  
585        *Remote Sensing and Spatial Information Sciences* XLVIII-3-2024,  
586        pp. 63–70. ISSN: 2194-9034. DOI: 10.5194/isprs-archives-xlviii-3-

- 587 2024-63-2024. URL: <http://dx.doi.org/10.5194/ISPRS-ARCHIVES-XLVIII-3-2024-63-2024>.
- 588
- 589 Choe, Hyeyeong, Junhwa Chi, and James H. Thorne (June 2021). “Mapping  
590 Potential Plant Species Richness over Large Areas with Deep Learning,  
591 MODIS, and Species Distribution Models”. In: *Remote Sensing* 13.13,  
592 p. 2490. ISSN: 2072-4292. DOI: 10.3390/rs13132490. URL: <http://dx.doi.org/10.3390/rs13132490>.
- 593
- 594 Cohen, Jacob (Apr. 1960). “A Coefficient of Agreement for Nominal Scales”.  
595 In: *Educational and Psychological Measurement* 20.1, pp. 37–46. ISSN:  
596 1552-3888. DOI: 10.1177/001316446002000104. URL: <http://dx.doi.org/10.1177/001316446002000104>.
- 597
- 598 Conrad, Felix, Mauritz Mälzer, Michael Schwarzenberger, Hajo Wiemer, and  
599 Steffen Ihlenfeldt (Nov. 2022). “Benchmarking AutoML for regression  
600 tasks on small tabular data in materials design”. In: *Scientific Reports*  
601 12.1. ISSN: 2045-2322. DOI: 10.1038/s41598-022-23327-1. URL: <http://dx.doi.org/10.1038/s41598-022-23327-1>.
- 602
- 603 De Marco, Paulo and Caroline Corrêa Nóbrega (Sept. 2018). “Evaluating  
604 collinearity effects on species distribution models: An approach based on  
605 virtual species simulation”. In: *PLOS ONE* 13.9. Ed. by Luciano Bosso,  
606 e0202403. ISSN: 1932-6203. DOI: 10.1371/journal.pone.0202403. URL:  
607 <http://dx.doi.org/10.1371/journal.pone.0202403>.
- 608
- 609 Dormann, Carsten F., Jane Elith, Sven Bacher, Carsten Buchmann, Gu-  
drun Carl, Gabriel Carré, Jaime R. García Marquéz, Bernd Gruber,

- 610 Bruno Lafourcade, Pedro J. Leitão, Tamara Münkemüller, Colin Mc-  
611 Clean, Patrick E. Osborne, Björn Reineking, Boris Schröder, Andrew K.  
612 Skidmore, Damaris Zurell, and Sven Lautenbach (May 2012). “Collinearity:  
613 a review of methods to deal with it and a simulation study evaluating  
614 their performance”. In: *Ecography* 36.1, pp. 27–46. ISSN: 1600-0587. DOI:  
615 [10.1111/j.1600-0587.2012.07348.x](https://doi.org/10.1111/j.1600-0587.2012.07348.x). URL: <http://dx.doi.org/10.1111/j.1600-0587.2012.07348.x>.
- 616
- 617 Edwards, Charles T. T., Kathleen S. Gobush, Fiona Maisels, Dave Balfour,  
618 Russell Taylor, and George Wittemyer (Nov. 2024). “Survey-based in-  
619 ference of continental African elephant decline”. In: *Proceedings of the*  
620 *National Academy of Sciences* 121.48. ISSN: 1091-6490. DOI: [10.1073/pnas.2403816121](https://doi.org/10.1073/pnas.2403816121). URL: <http://dx.doi.org/10.1073/pnas.2403816121>.
- 621
- 622 Elith, Jane and John R. Leathwick (Dec. 2009). “Species Distribution Models:  
623 Ecological Explanation and Prediction Across Space and Time”. In: *Annual*  
624 *Review of Ecology, Evolution, and Systematics* 40.1, pp. 677–697. ISSN:  
625 1545-2069. DOI: [10.1146/annurev.ecolsys.110308.120159](https://doi.org/10.1146/annurev.ecolsys.110308.120159). URL: <http://dx.doi.org/10.1146/ANNUREV.ECOLSYS.110308.120159>.
- 626
- 627 Estopinan, Joaquim, Maximilien Servajean, Pierre Bonnet, François Munoz,  
628 and Alexis Joly (Apr. 2022). “Deep Species Distribution Modeling From  
629 Sentinel-2 Image Time-Series: A Global Scale Analysis on the Orchid  
630 Family”. In: *Frontiers in Plant Science* 13. ISSN: 1664-462X. DOI: [10.3389/fpls.2022.839327](https://doi.org/10.3389/fpls.2022.839327). URL: <http://dx.doi.org/10.3389/fpls.2022.839327>.
- 631
- 632

- 633 Fawcett, Tom (June 2006). “An introduction to ROC analysis”. In: *Pattern*  
634      *Recognition Letters* 27.8, pp. 861–874. ISSN: 0167-8655. DOI: 10.1016/j.  
635      patrec.2005.10.010. URL: <http://dx.doi.org/10.1016/j.patrec.2005.10.010>.
- 636 Feng, Xiao, Daniel S. Park, Ye Liang, Ranjit Pandey, and Monica Papes  
637      (Aug. 2019). “Collinearity in ecological niche modeling: Confusions and  
638      challenges”. In: *Ecology and Evolution* 9.18, pp. 10365–10376. ISSN: 2045-  
639      7758. DOI: 10.1002/ece3.5555. URL: <http://dx.doi.org/10.1002/ece3.5555>.
- 640 Feurer, Matthias, Katharina Eggensperger, Stefan Falkner, Marius Lindauer,  
641      and Frank Hutter (2020). “Auto-sklearn 2.0: The Next Generation”. In:  
642      *Proceedings of the AutoML Conference 2020*. URL: [https://www.automl.org/wp-content/uploads/2020/07/AutoML\\_2020\\_paper\\_61.pdf](https://www.automl.org/wp-content/uploads/2020/07/AutoML_2020_paper_61.pdf).
- 643 Feurer, Matthias and Frank Hutter (2019). “Hyperparameter Optimization”.  
644      In: *Automated Machine Learning*. Springer International Publishing, pp. 3–  
645      33. ISBN: 9783030053185. DOI: 10.1007/978-3-030-05318-5\_1. URL:  
646      [http://dx.doi.org/10.1007/978-3-030-05318-5\\_1](http://dx.doi.org/10.1007/978-3-030-05318-5_1).
- 647 Fieberg, John, Johannes Signer, Brian Smith, and Tal Avgar (Mar. 2021). “A  
648      ‘How to’ guide for interpreting parameters in habitat-selection analyses”.  
649      In: *Journal of Animal Ecology* 90.5, pp. 1027–1043. ISSN: 1365-2656. DOI:  
650      10.1111/1365-2656.13441. URL: <http://dx.doi.org/10.1111/1365-2656.13441>.

- 655 Fischer, Joern and David B. Lindenmayer (Feb. 2007). “Landscape modifi-  
656 cation and habitat fragmentation: a synthesis”. In: *Global Ecology and*  
657 *Biogeography* 16.3, pp. 265–280. ISSN: 1466-8238. DOI: 10.1111/j.1466-  
658 8238.2007.00287.x. URL: <http://dx.doi.org/10.1111/j.1466-8238.2007.00287.x>.
- 660 Fleiss, Joseph L., Bruce Levin, and Myunghee Cho Paik (Sept. 2003). *Statis-  
661 tical Methods for Rates and Proportions*. Wiley. ISBN: 9780471445425. DOI:  
662 10.1002/0471445428. URL: <http://dx.doi.org/10.1002/0471445428>.
- 663 Frantz, Bethany H., Maritza Sepúlveda, Marisol García-Reyes, Rodrigo Vega,  
664 Daniel M. Palacios, Luis Bedriñana-Romano, Luis A. Hückstädt, Macarena  
665 Santos-Carvallo, Jerry D. Davis, and Ellen Hines (June 2024). “Combining  
666 potential and realized distribution modeling of telemetry data for a bycatch  
667 risk assessment”. In: *Ecology and Evolution* 14.6. ISSN: 2045-7758. DOI:  
668 10.1002/ece3.11541. URL: <http://dx.doi.org/10.1002/ece3.11541>.
- 669 Friswold, Brooke, Brett Mitchell, George Gale, and Antoinette Van de Water  
670 (Nov. 2023). “Twisting collars on male elephants in shrub terrain: animal  
671 welfare considerations for researchers, managers and manufacturers”. In:  
672 *Pachyderm* 64, pp. 78–91. ISSN: 1026-2881. DOI: 10.69649/pachyderm.  
673 v64i.534. URL: <http://dx.doi.org/10.69649/pachyderm.v64i.534>.
- 674 Fuchs, Matthias and Wolfram Höpken (2022). “Clustering: Hierarchical, k-  
675 Means, DBSCAN”. In: *Applied Data Science in Tourism*. Springer Interna-  
676 tional Publishing, pp. 129–149. ISBN: 9783030883898. DOI: 10.1007/978-

- 677 3-030-88389-8\_8. URL: [http://dx.doi.org/10.1007/978-3-030-88389-8\\_8](http://dx.doi.org/10.1007/978-3-030-88389-8_8).
- 678 Gaber, Max, Yanghui Kang, Guy Schurgers, and Trevor Keenan (May 2024).
- 680 “Using automated machine learning for the upscaling of gross primary
- 681 productivity”. In: *Biogeosciences* 21.10, pp. 2447–2472. ISSN: 1726-4189.
- 682 DOI: 10.5194/bg-21-2447-2024. URL: <http://dx.doi.org/10.5194/bg-21-2447-2024>.
- 683 Giliba, Richard A., Christian Kiffner, Pascal Fust, and Jacqueline Loos (Oct. 2023). “Modelling elephant corridors over two decades reveals opportunities for conserving connectivity across a large protected area network”. In: *PLOS ONE* 18.10. Ed. by Daniel de Paiva Silva, e0292918. ISSN: 1932-6203.
- 688 DOI: 10.1371/journal.pone.0292918. URL: <http://dx.doi.org/10.1371/journal.pone.0292918>.
- 690 Gilman, Eric and Milani Chaloupka (Feb. 2024). “Evidence from interpretable
- 691 machine learning to inform spatial management of Palau’s tuna fisheries”.
- 692 In: *Ecosphere* 15.2. ISSN: 2150-8925. DOI: 10.1002/ecs2.4751. URL:
- 693 <http://dx.doi.org/10.1002/ecs2.4751>.
- 694 Grass, Ingo, Jacqueline Loos, Svenja Baensch, Péter Batáry, Felipe Librán-
- 695 Embid, Anoush Ficiciyan, Felix Klaus, Maraja Riechers, Julia Rosa,
- 696 Julia Tiede, Kristy Udy, Catrin Westphal, Annemarie Wurz, and Teja
- 697 Tscharntke (Apr. 2019). “Land-sharing/-sparing connectivity landscapes
- 698 for ecosystem services and biodiversity conservation”. In: *People and Na-*

- 699       ture 1.2, pp. 262–272. ISSN: 2575-8314. DOI: 10.1002/pan3.21. URL:  
700       <http://dx.doi.org/10.1002/pan3.21>.
- 701       Gross, Michael (Jan. 2024). “Of elephants and men”. In: *Current Biology* 34.2,  
702       R37–R40. ISSN: 0960-9822. DOI: 10.1016/j.cub.2024.01.001. URL:  
703       <http://dx.doi.org/10.1016/j.cub.2024.01.001>.
- 704       Guisan, Antoine, Reid Tingley, John B. Baumgartner, Ilona Naujokaitis-  
705       Lewis, Patricia R. Sutcliffe, Ayesha I. T. Tulloch, Tracey J. Regan, Lluis  
706       Brotons, Eve McDonald-Madden, Chrystal Mantyka-Pringle, Tara G.  
707       Martin, Jonathan R. Rhodes, Ramona Maggini, Samantha A. Setterfield,  
708       Jane Elith, Mark W. Schwartz, Brendan A. Wintle, Olivier Broennimann,  
709       Mike Austin, Simon Ferrier, Michael R. Kearney, Hugh P. Possingham,  
710       and Yvonne M. Buckley (Oct. 2013). “Predicting species distributions for  
711       conservation decisions”. In: *Ecology Letters* 16.12. Ed. by Hector Arita,  
712       pp. 1424–1435. ISSN: 1461-0248. DOI: 10.1111/ele.12189. URL: <http://dx.doi.org/10.1111/ele.12189>.
- 713
- 714       Guisan, Antoine and Niklaus E. Zimmermann (Dec. 2000). “Predictive habitat  
715       distribution models in ecology”. In: *Ecological Modelling* 135.2–3, pp. 147–  
716       186. ISSN: 0304-3800. DOI: 10.1016/S0304-3800(00)00354-9. URL:  
717       [http://dx.doi.org/10.1016/S0304-3800\(00\)00354-9](http://dx.doi.org/10.1016/S0304-3800(00)00354-9).
- 718       H2O.ai (2024). *H2O AutoML User Guide*. Accessed: 2024-11-30. URL: <https://docs.h2o.ai/h2o/latest-stable/h2o-docs/automl.html>.
- 719
- 720       Hahsler, Michael, Matthew Piekenbrock, and Derek Doran (2019). “dbscan:  
721       Fast Density-Based Clustering with R”. In: *Journal of Statistical Software*

- 722 91.1. ISSN: 1548-7660. DOI: 10.18637/jss.v091.i01. URL: <http://dx.doi.org/10.18637/JSS.V091.I01>.
- 723
- 724 Hebblewhite, Mark and Daniel T. Haydon (July 2010). “Distinguishing technology from biology: a critical review of the use of GPS telemetry data in ecology”. In: *Philosophical Transactions of the Royal Society B: Biological Sciences* 365.1550, pp. 2303–2312. ISSN: 1471-2970. DOI: 10.1098/rstb.2010.0087. URL: <http://dx.doi.org/10.1098/rstb.2010.0087>.
- 725
- 726
- 727
- 728
- 729 Hesselbarth, Maximilian H. K., Jakub Nowosad, Alida de Flamingh, Craig E.
- 730 Simpkins, Martin Jung, Gemma Gerber, and Martí Bosch (Dec. 2024).
- 731 “Computational Methods in Landscape Ecology”. In: *Current Landscape*
- 732 *Ecology Reports* 10.1. ISSN: 2364-494X. DOI: 10.1007/s40823-024-00104-
- 733 6. URL: <http://dx.doi.org/10.1007/s40823-024-00104-6>.
- 734 Hönisch, Bärbel, Dana L. Royer, Daniel O. Breecker, Pratigya J. Polissar,
- 735 Gabriel J. Bowen, Michael J. Henehan, Ying Cui, Margret Steinhorsdottir,
- 736 Jennifer C. McElwain, Matthew J. Kohn, Ann Pearson, Samuel R. Phelps,
- 737 Kevin T. Uno, Andy Ridgwell, Eleni Anagnostou, Jacqueline Austermann,
- 738 Marcus P. S. Badger, Richard S. Barclay, Peter K. Bijl, Thomas B. Chalk,
- 739 Christopher R. Scotese, Elwyn de la Vega, Robert M. DeConto, Kelsey A.
- 740 Dyez, Vicki Ferrini, Peter J. Franks, Claudia F. Giulivi, Marcus Gutjahr,
- 741 Dustin T. Harper, Laura L. Haynes, Matthew Huber, Kathryn E. Snell,
- 742 Benjamin A. Keisling, Wilfried Konrad, Tim K. Lowenstein, Alberto
- 743 Malinverno, Maxence Guillermic, Luz María Mejía, Joseph N. Milligan,
- 744 John J. Morton, Lee Nordt, Ross Whiteford, Anita Roth-Nebelsick, Jeremy

745 K. C. Rugenstein, Morgan F. Schaller, Nathan D. Sheldon, Sindia Sosdian,  
746 Elise B. Wilkes, Caitlyn R. Witkowski, Yi Ge Zhang, Lloyd Anderson,  
747 David J. Beerling, Clara Bolton, Thure E. Cerling, Jennifer M. Cotton,  
748 Jiawei Da, Douglas D. Ekart, Gavin L. Foster, David R. Greenwood, Ethan  
749 G. Hyland, Elliot A. Jagniecki, John P. Jasper, Jennifer B. Kowalczyk, Lutz  
750 Kunzmann, Wolfram M. Kürschner, Charles E. Lawrence, Caroline H. Lear,  
751 Miguel A. Martínez-Botí, Daniel P. Maxbauer, Paolo Montagna, B. David  
752 A. Naafs, James W. B. Rae, Markus Raitzsch, Gregory J. Retallack, Simon  
753 J. Ring, Osamu Seki, Julio Sepúlveda, Ashish Sinha, Tekie F. Tesfamichael,  
754 Aradhna Tripati, Johan van der Burgh, Jimin Yu, James C. Zachos, and  
755 Laiming Zhang (Dec. 2023). “Toward a Cenozoic history of atmospheric CO  
756 2”. In: *Science* 382.6675. ISSN: 1095-9203. DOI: 10.1126/science.ad15177.  
757 URL: <http://dx.doi.org/10.1126/science.ad15177>.

758 Jochems, Louis, Jodi Brandt, Clayton Kingdon, Samuel J. Schurkamp, Andrew  
759 Monks, and Shane C. Lishawa (Nov. 2024). “Active remote sensing data  
760 and dispersal processes improve predictions for an invasive aquatic plant  
761 during a climatic extreme in Great Lakes coastal wetlands”. In: *Journal*  
762 *of Environmental Management* 370, p. 122610. ISSN: 0301-4797. DOI:  
763 10.1016/j.jenvman.2024.122610. URL: <http://dx.doi.org/10.1016/j.jenvman.2024.122610>.

764 Karp, Melissa A, Megan Cimino, J Kevin Craig, Daniel P Crear, Christo-  
765 pher Haak, Elliott L Hazen, Isaac Kaplan, Donald R Kobayashi, Hassan  
766 Moustahfid, Barbara Muhling, Malin L Pinsky, Laurel A Smith, James T  
767

- 768 Thorson, and Phoebe A Woodworth-Jefcoats (Mar. 2025). “Applications  
769 of species distribution modeling and future needs to support marine re-  
770 source management”. In: *ICES Journal of Marine Science* 82.3. Ed. by  
771 Anita Gilles. ISSN: 1095-9289. DOI: 10.1093/icesjms/fsaf024. URL:  
772 <http://dx.doi.org/10.1093/icesjms/fsaf024>.
- 773 Kass, Jamie M., Adam B. Smith, Dan L. Warren, Sergio Vignali, Sylvain  
774 Schmitt, Matthew E. Aiello-Lammens, Eduardo Arlé, Ana Márcia Barbosa,  
775 Olivier Broennimann, Marlon E. Cobos, Maya Guéguen, Antoine Guisan,  
776 Cory Merow, Babak Naimi, Michael P. Nobis, Ian Ondo, Luis Osorio-  
777 Olvera, Hannah L. Owens, Gonzalo E. Pinilla-Buitrago, Andrea Sánchez-  
778 Tapia, Wilfried Thuiller, Roozbeh Valavi, Santiago José Elías Velazco,  
779 Alexander Zizka, and Damaris Zurell (Nov. 2024). “Achieving higher  
780 standards in species distribution modeling by leveraging the diversity of  
781 available software”. In: *Ecography* 2025.2. ISSN: 1600-0587. DOI: 10.1111/  
782 <http://dx.doi.org/10.1111/ecog.07346>. URL: <http://dx.doi.org/10.1111/ecog.07346>.
- 783 Kau, Minyi, Byron V. Weckworth, Sheng Li, Mathias M. Pires, Daiying Jin,  
784 Michela Pacifici, Carlo Rondinini, Luigi Boitani, Thomas M. McCarthy,  
785 Zhi Lu, George B. Schaller, Steven R. Beissinger, and Juan Li (Mar.  
786 2025). “Umbrella, keystone, or flagship? An integrated framework for  
787 identifying effective surrogate species”. In: *Biological Conservation* 303,  
788 p. 111025. ISSN: 0006-3207. DOI: 10.1016/j.biocon.2025.111025. URL:  
789 <http://dx.doi.org/10.1016/j.biocon.2025.111025>.

- 790 Kindt, R. (Feb. 2018). “Ensemble species distribution modelling with trans-  
791 formed suitability values”. In: *Environmental Modelling & Software* 100,  
792 pp. 136–145. ISSN: 1364-8152. DOI: 10.1016/j.envsoft.2017.11.009.  
793 URL: <http://dx.doi.org/10.1016/J.ENVSOFT.2017.11.009>.
- 794 Konowalik, Kamil and Agata Nosol (Jan. 2021). “Evaluation metrics and  
795 validation of presence-only species distribution models based on distri-  
796 butional maps with varying coverage”. In: *Scientific Reports* 11.1. ISSN:  
797 2045-2322. DOI: 10.1038/s41598-020-80062-1. URL: <http://dx.doi.org/10.1038/s41598-020-80062-1>.
- 799 Kremen, Claire (July 2015). “Reframing the land-sparing/land-sharing debate  
800 for biodiversity conservation”. In: *Annals of the New York Academy of  
801 Sciences* 1355.1, pp. 52–76. ISSN: 1749-6632. DOI: 10.1111/nyas.12845.  
802 URL: <http://dx.doi.org/10.1111/nyas.12845>.
- 803 Kumari, Annu and S. Karthikeyan (Oct. 2023). “Sentinel-2 Data for Land  
804 Use/Land Cover Mapping: A Meta-analysis and Review”. In: *SN Computer  
805 Science* 4.6. ISSN: 2661-8907. DOI: 10.1007/s42979-023-02214-0. URL:  
806 <http://dx.doi.org/10.1007/s42979-023-02214-0>.
- 807 Loarie, Scott R., Rudi J. van Aarde, and Stuart L. Pimm (Dec. 2009). “Ele-  
808 phant seasonal vegetation preferences across dry and wet savannas”. In:  
809 *Biological Conservation* 142.12, pp. 3099–3107. ISSN: 0006-3207. DOI:  
810 10.1016/j.biocon.2009.08.021. URL: <http://dx.doi.org/10.1016/j.biocon.2009.08.021>.

- 812 Maitner, Brian S., Robert L. Richards, Ben Carlson, John M. Drake, and Cory  
813 Merow (Apr. 2025). “Flexible Methods for Species Distribution Modeling  
814 with Small Samples”. In: *bioRxiv*. DOI: 10.1101/2025.04.03.647025.  
815 eprint: <https://www.biorxiv.org/content/early/2025/04/08/2025.04.03.647025.full.pdf>. URL: <http://dx.doi.org/10.1101/2025.04.03.647025>.
- 816
- 817
- 818 Matthiopoulos, Jason, John Fieberg, Geert Aarts, Hawthorne L. Beyer, Juan  
819 M. Morales, and Daniel T. Haydon (Aug. 2015). “Establishing the link  
820 between habitat selection and animal population dynamics”. In: *Ecological  
821 Monographs* 85.3, pp. 413–436. ISSN: 1557-7015. DOI: 10.1890/14-2244.1.  
822 URL: <http://dx.doi.org/10.1890/14-2244.1>.
- 823 Naha, Dipanjan, Stéphanie Périquet, J. Werner Kilian, Caitlin A. Kupferman,  
824 Tammy Hoth-Hanssen, and James C. Beasley (June 2023). “Fencing af-  
825 fects movement patterns of two large carnivores in Southern Africa”. In:  
826 *Frontiers in Ecology and Evolution* 11. ISSN: 2296-701X. DOI: 10.3389/  
827 fevo.2023.1031321. URL: <http://dx.doi.org/10.3389/fevo.2023.1031321>.
- 828
- 829 Naidoo, Robin, Cody Aylward, Wendy Elliott, Annika Keeley, Margaret  
830 Kinnaird, Michael Knight, Cristian-Remus Papp, Kanchan Thapa, and  
831 Rafael Antelo (July 2025). “From science to impact: Conserving ecological  
832 connectivity in large conservation landscapes”. In: *Proceedings of the  
833 National Academy of Sciences* 122.31. ISSN: 1091-6490. DOI: 10.1073/pnas.  
834 2410937122. URL: <http://dx.doi.org/10.1073/pnas.2410937122>.

- 835 Nampindo, Simon and Timothy O. Randhir (Jan. 2024). "Dynamic modeling  
836 of African elephant populations under changing climate and habitat loss  
837 across the Greater Virunga Landscape". In: *PLOS Sustainability and*  
838 *Transformation* 3.1. Ed. by Alka Bharat, e0000094. ISSN: 2767-3197. DOI:  
839 10.1371/journal.pstr.0000094. URL: <http://dx.doi.org/10.1371/journal.pstr.0000094>.
- 841 Omar, Intisar, Muhammad Khan, Andrew Starr, and Khaled Abou Rok Ba  
842 (Oct. 2023). "Automated Prediction of Crack Propagation Using H2O  
843 AutoML". In: *Sensors* 23.20, p. 8419. ISSN: 1424-8220. DOI: 10.3390/  
844 s23208419. URL: <http://dx.doi.org/10.3390/s23208419>.
- 845 Osipova, Liudmila, Moses M. Okello, Steven J. Njumbi, Shadrack Ngene,  
846 David Western, Matt W. Hayward, and Niko Balkenhol (Aug. 2018).  
847 "Fencing solves human-wildlife conflict locally but shifts problems else-  
848 where: A case study using functional connectivity modelling of the African  
849 elephant". In: *Journal of Applied Ecology* 55.6. Ed. by Matthew Struebig,  
850 pp. 2673–2684. ISSN: 1365-2664. DOI: 10.1111/1365-2664.13246. URL:  
851 <http://dx.doi.org/10.1111/1365-2664.13246>.
- 852 Pacifici, Michela, Piero Visconti, Stuart H. M. Butchart, James E. M. Watson,  
853 Francesca M. Cassola, and Carlo Rondinini (Feb. 2017). "Species' traits  
854 influenced their response to recent climate change". In: *Nature Climate  
855 Change* 7.3, pp. 205–208. ISSN: 1758-6798. DOI: 10.1038/nclimate3223.  
856 URL: <http://dx.doi.org/10.1038/nclimate3223>.

- 857 Phillips, Steven J. and Miroslav Dudík (Mar. 2008). "Modeling of species dis-  
858 tributions with Maxent: new extensions and a comprehensive evaluation".  
859 In: *Ecography* 31.2, pp. 161–175. ISSN: 1600-0587. DOI: 10.1111/j.0906-  
860 7590 . 2008 . 5203 . x. URL: <http://dx.doi.org/10.1111/J.0906-7590.2008.5203.X>.
- 861
- 862 Pontius, Robert Gilmore and Marco Millones (Aug. 2011). "Death to Kappa:  
863 birth of quantity disagreement and allocation disagreement for accuracy  
864 assessment". In: *International Journal of Remote Sensing* 32.15, pp. 4407–  
865 4429. ISSN: 1366-5901. DOI: 10 . 1080 / 01431161 . 2011 . 552923. URL:  
866 <http://dx.doi.org/10.1080/01431161.2011.552923>.
- 867
- 868 Ratajczak, Zak, Scott L. Collins, John M. Blair, Sally E. Koerner, Allison  
869 M. Louthan, Melinda D. Smith, Jeffrey H. Taylor, and Jesse B. Nippert  
870 (Aug. 2022). "Reintroducing bison results in long-running and resilient  
871 increases in grassland diversity". In: *Proceedings of the National Academy  
872 of Sciences* 119.36. ISSN: 1091-6490. DOI: 10 . 1073 / pnas . 2210433119.  
873 URL: <http://dx.doi.org/10.1073/pnas.2210433119>.
- 874
- 875 Rausell-Moreno, Armand, Núria Galiana, Babak Naimi, and Miguel B. Araújo  
876 (Aug. 2025). "Improving species distribution models by optimising back-  
877 ground points: Impacts on current and future climate projections". In:  
878 *Ecological Modelling* 507, p. 111177. ISSN: 0304-3800. DOI: 10 . 1016 /  
j . ecolmodel . 2025 . 111177. URL: <http://dx.doi.org/10.1016/j.ecolmodel.2025.111177>.

- 879 Real, Raimundo and Juan M. Vargas (Sept. 1996). “The Probabilistic Basis of  
880 Jaccard’s Index of Similarity”. In: *Systematic Biology* 45.3. Ed. by Richard  
881 Olmstead, pp. 380–385. ISSN: 1063-5157. DOI: 10.1093/sysbio/45.3.380.  
882 URL: <http://dx.doi.org/10.1093/sysbio/45.3.380>.
- 883 Riva, Federico, Caroline Jean Martin, Carmen Galán Acedo, Erwan Nicolas  
884 Bellon, Petr Keil, Alejandra Morán-Ordóñez, Lenore Fahrig, and Antoine  
885 Guisan (Aug. 2024). “Incorporating effects of habitat patches into species  
886 distribution models”. In: *Journal of Ecology* 112.10, pp. 2162–2182. ISSN:  
887 1365-2745. DOI: 10.1111/1365-2745.14403. URL: <http://dx.doi.org/10.1111/1365-2745.14403>.
- 888
- 889 Roberts, David R., Volker Bahn, Simone Ciuti, Mark S. Boyce, Jane Elith,  
890 Gurutzeta Guillera-Arroita, Severin Hauenstein, José J. Lahoz-Monfort,  
891 Boris Schröder, Wilfried Thuiller, David I. Warton, Brendan A. Wintle,  
892 Florian Hartig, and Carsten F. Dormann (Mar. 2017). “Cross-validation  
893 strategies for data with temporal, spatial, hierarchical, or phylogenetic  
894 structure”. In: *Ecography* 40.8, pp. 913–929. ISSN: 1600-0587. DOI: 10.  
895 1111/ecog.02881. URL: <http://dx.doi.org/10.1111/ecog.02881>.
- 896 Schmitt, Sylvain, Robin Pouteau, Dimitri Justeau, Florian de Boissieu, and  
897 Philippe Birnbaum (Aug. 2017). “<scp>ssdm</scp>: An <scp>r</scp>  
898 package to predict distribution of species richness and composition based on  
899 stacked species distribution models”. In: *Methods in Ecology and Evolution*  
900 8.12. Ed. by Nick Golding, pp. 1795–1803. ISSN: 2041-210X. DOI: 10.

- 901        1111/2041-210x . 12841. URL: <http://dx.doi.org/10.1111/2041->  
902        210X.12841.
- 903        Schurr, Frank M., Jörn Pagel, Juliano Sarmento Cabral, Jürgen Groeneveld,  
904        Olga Bykova, Robert B. O'Hara, Florian Hartig, W. Daniel Kissling,  
905        H. Peter Linder, Guy F. Midgley, Boris Schröder, Alexander Singer, and  
906        Niklaus E. Zimmermann (Aug. 2012). "How to understand species' niches  
907        and range dynamics: a demographic research agenda for biogeography".  
908        In: *Journal of Biogeography* 39.12, pp. 2146–2162. ISSN: 1365-2699. DOI:  
909        10.1111/j.1365-2699.2012.02737.x. URL: <http://dx.doi.org/10.1111/j.1365-2699.2012.02737.x>.
- 910        Schwandner, Imogen A., Thomas A. Morrison, J. Grant C. Hopcraft, Jake  
911        Wall, Lacey Hughey, Randall B. Boone, Joseph O. Ogutu, Andrew F.  
912        Jakes, Shem C. Kifugo, Campaign Limo, Stephen Ndambuki Mwiu, Vasco  
913        Nyaga, Han Olff, Gordon O. Ojwang, Wilson Sairowua, Jackson Sasine,  
914        Jully S. Senteu, Daniel Sopia, Jeffrey Worden, and Jared A. Stabach (Jan.  
915        2025). "Predicting the impact of targeted fence removal on connectivity in  
916        a migratory ecosystem". In: *Ecological Applications* 35.1. ISSN: 1939-5582.  
917        DOI: 10.1002/eap.3094. URL: <http://dx.doi.org/10.1002/eap.3094>.
- 918        Somers, Robert H. (1962). "A New Asymmetric Measure of Association  
919        for Ordinal Variables". In: *American Sociological Review* 27.6. JSTOR  
920        Stable URL <https://www.jstor.org/stable/2090408>, pp. 799–811. DOI:  
921        10.2307/2090406. URL: <https://doi.org/10.2307/2090408>.

- 923 Stasinou, Stylianos, Martino Mensio, Elena Lazovik, and Athanasios Trantas  
924 (2025). *BioCube: A Multimodal Dataset for Biodiversity Research*. arXiv:  
925 2505.11568 [q-bio.QM]. URL: <https://arxiv.org/abs/2505.11568>.
- 926 Sullivan, Lauren L., Adam T. Clark, David Tilman, and Allison K. Shaw  
927 (Oct. 2018). “Mechanistically derived dispersal kernels explain species-level  
928 patterns of recruitment and succession”. In: *Ecology* 99.11, pp. 2415–2420.  
929 ISSN: 1939-9170. DOI: 10.1002/ecy.2498. URL: <http://dx.doi.org/10.1002/ecy.2498>.
- 930 Syphard, Alexandra D. and Janet Franklin (Dec. 2009). “Differences in spatial  
931 predictions among species distribution modeling methods vary with species  
932 traits and environmental predictors”. In: *Ecography* 32.6, pp. 907–918.  
933 ISSN: 1600-0587. DOI: 10.1111/j.1600-0587.2009.05883.x. URL:  
934 <http://dx.doi.org/10.1111/J.1600-0587.2009.05883.X>.
- 935 Tian, Junchi and Chang Che (Dec. 2024). “Automated Machine Learning: A  
936 Survey of Tools and Techniques”. In: *Journal of Industrial Engineering  
937 and Applied Science* 2.6, pp. 71–76. ISSN: 3005-608X. DOI: 10.70393/  
938 6a69656173.323336. URL: <http://dx.doi.org/10.70393/6a69656173.323336>.
- 939 Timóteo, Sérgio, Jörg Albrecht, Beatriz Rumeu, Ana C. Norte, Anna Trav-  
940 eset, Carol M. Frost, Elizabete Marchante, Francisco A. López-Núñez,  
941 Guadalupe Peralta, Jane Memmott, Jens M. Olesen, José M. Costa, Luís  
942 P. da Silva, Luísa G. Carvalheiro, Marta Correia, Michael Staab, Nico  
943 Blüthgen, Nina Farwig, Sandra Hervías-Parejo, Sergei Mironov, Susana  
944

- 946 Rodríguez-Echeverría, and Ruben Heleno (Oct. 2022). “Tripartite networks  
947 show that keystone species can multitask”. In: *Functional Ecology* 37.2,  
948 pp. 274–286. ISSN: 1365-2435. DOI: 10.1111/1365-2435.14206. URL:  
949 <http://dx.doi.org/10.1111/1365-2435.14206>.
- 950 Tobias, Joseph A., James M. Bullock, Lynn V. Dicks, Brenna R. Forester, and  
951 Orly Razgour (July 2025). “Biodiversity conservation requires integration  
952 of species-centric and process-based strategies”. In: *Proceedings of the*  
953 *National Academy of Sciences* 122.31. ISSN: 1091-6490. DOI: 10.1073/pnas.  
954 2410936122. URL: <http://dx.doi.org/10.1073/pnas.2410936122>.
- 955 Tuiia, Devis, Benjamin Kellenberger, Sara Beery, Blair R. Costelloe, Silvia  
956 Zuffi, Benjamin Risse, Alexander Mathis, Mackenzie W. Mathis, Frank van  
957 Langevelde, Tilo Burghardt, Roland Kays, Holger Klinck, Martin Wikelski,  
958 Iain D. Couzin, Grant van Horn, Margaret C. Crofoot, Charles V. Stewart,  
959 and Tanya Berger-Wolf (Feb. 2022). “Perspectives in machine learning for  
960 wildlife conservation”. In: *Nature Communications* 13.1. ISSN: 2041-1723.  
961 DOI: 10.1038/s41467-022-27980-y. URL: <http://dx.doi.org/10.1038/s41467-022-27980-y>.
- 962 Valavi, Roozbeh, Jane Elith, José J. Lahoz-Monfort, and Gurutzeta Guillera-  
963 Arroita (Nov. 2018). “<scp>block</scp><scp>CV</scp>: An <scp>r</scp>  
964 package for generating spatially or environmentally separated folds for  
965 k-fold cross-validation of species distribution models”. In: *Methods in*  
966 *Ecology and Evolution* 10.2. Ed. by David Warton, pp. 225–232. ISSN:  
967

- 968        2041-210X. DOI: 10.1111/2041-210x.13107. URL: <http://dx.doi.org/10.1111/2041-210X.13107>.
- 969
- 970        Van de Water, Antoinette, Marion Garaï, Matthew Burnett, Michelle Hen-
- 971        ley, Enrico Di Minin, Jarryd Streicher, Lucy Bates, and Rob Slotow
- 972        (2024). “Integrating a “One Well-being” approach in elephant conservation:
- 973        evaluating consequences of management interventions”. In: *Ecology and*
- 974        *Society* 29.3. ISSN: 1708-3087. DOI: 10.5751/es-15193-290315. URL:
- 975        <http://dx.doi.org/10.5751/ES-15193-290315>.
- 976        Vulcan Inc. (2025). *EarthRanger software*. Software, data monitored via LoRa
- 977        system. URL: <https://earthranger.com/>.
- 978        Wall, Jake, George Wittemyer, Brian Klinkenberg, and Iain Douglas-Hamilton
- 979        (June 2014). “Novel opportunities for wildlife conservation and research
- 980        with real-time monitoring”. In: *Ecological Applications* 24.4, pp. 593–601.
- 981        ISSN: 1939-5582. DOI: 10.1890/13-1971.1. URL: <http://dx.doi.org/10.1890/13-1971.1>.
- 982
- 983        Wang, Le, Chunyuan Diao, and Ying Lu (Nov. 2024). “The role of remote
- 984        sensing in species distribution models: a review”. In: *International Jour-*
- 985        *nal of Remote Sensing* 46.2, pp. 661–685. ISSN: 1366-5901. DOI: 10.
- 986        1080/01431161.2024.2421949. URL: <http://dx.doi.org/10.1080/01431161.2024.2421949>.
- 987
- 988        Wilkinson, Caitlin, Ulrich Brose, Alexander Dyer, Myriam R. Hirt, and
- 989        Remo Ryser (Feb. 2025). “A Mechanistic Approach to Animal Disper-
- 990        sal—Quantifying Energetics and Maximum Distances”. In: *Ecology Letters*

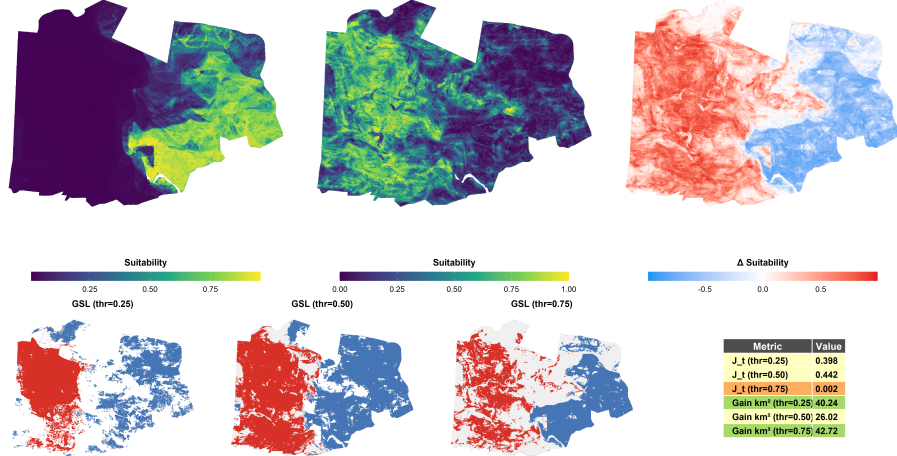
28.2. ISSN: 1461-0248. DOI: 10.1111/ele.70085. URL: <http://dx.doi.org/10.1111/ele.70085>.

Zurell, Damaris, Janet Franklin, Christian König, Phil J. Bouchet, Carsten F. Dormann, Jane Elith, Guillermo Fandos, Xiao Feng, Gurutzeta Guillera-Arroita, Antoine Guisan, José J. Lahoz-Monfort, Pedro J. Leitão, Daniel S. Park, A. Townsend Peterson, Giovanni Rapacciuolo, Dirk R. Schmaltz, Boris Schröder, Josep M. Serra-Diaz, Wilfried Thuiller, Katherine L. Yates, Niklaus E. Zimmermann, and Cory Merow (June 2020). “A standard protocol for reporting species distribution models”. In: *Ecography* 43.9, pp. 1261–1277. ISSN: 1600-0587. DOI: 10.1111/ecog.04960. URL: <http://dx.doi.org/10.1111/ecog.04960>.

## 6 Appendix

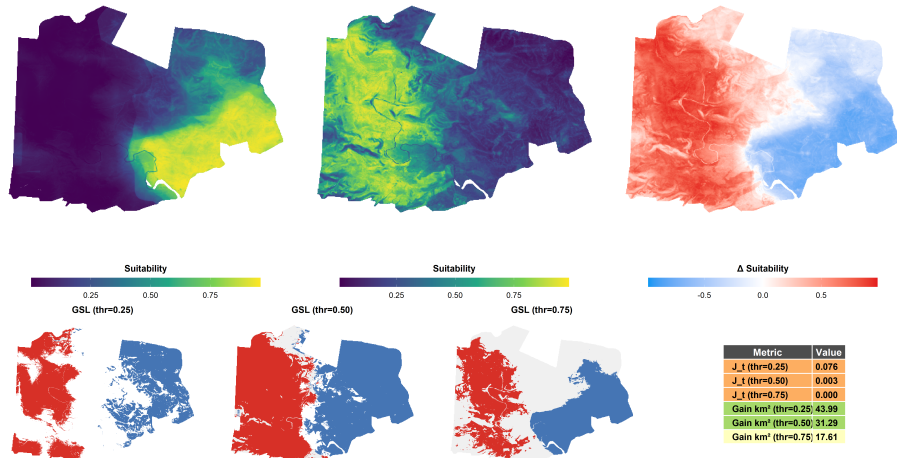
6.1 Per-elephant panel alignment of H<sub>2</sub>O AutoML (top) and SSDM (bottom) results for comparison of habitat change.

Elephant E4 — H<sub>2</sub>O | Before vs After: base maps,  $\Delta$  (A-B), GSL strip, temporal metrics



(a) E4 — H<sub>2</sub>O AutoML

Elephant E4 — SSDM | Before vs After: base maps,  $\Delta$  (A-B), GSL strip, temporal metrics



(b) E4 — SSDM

Figure 12: Per-elephant comparison for Half Moon (E4). The H<sub>2</sub>O AutoML and SSDM frameworks are shown vertically, highlighting contrasts in post-fence suitability patterns and change maps.

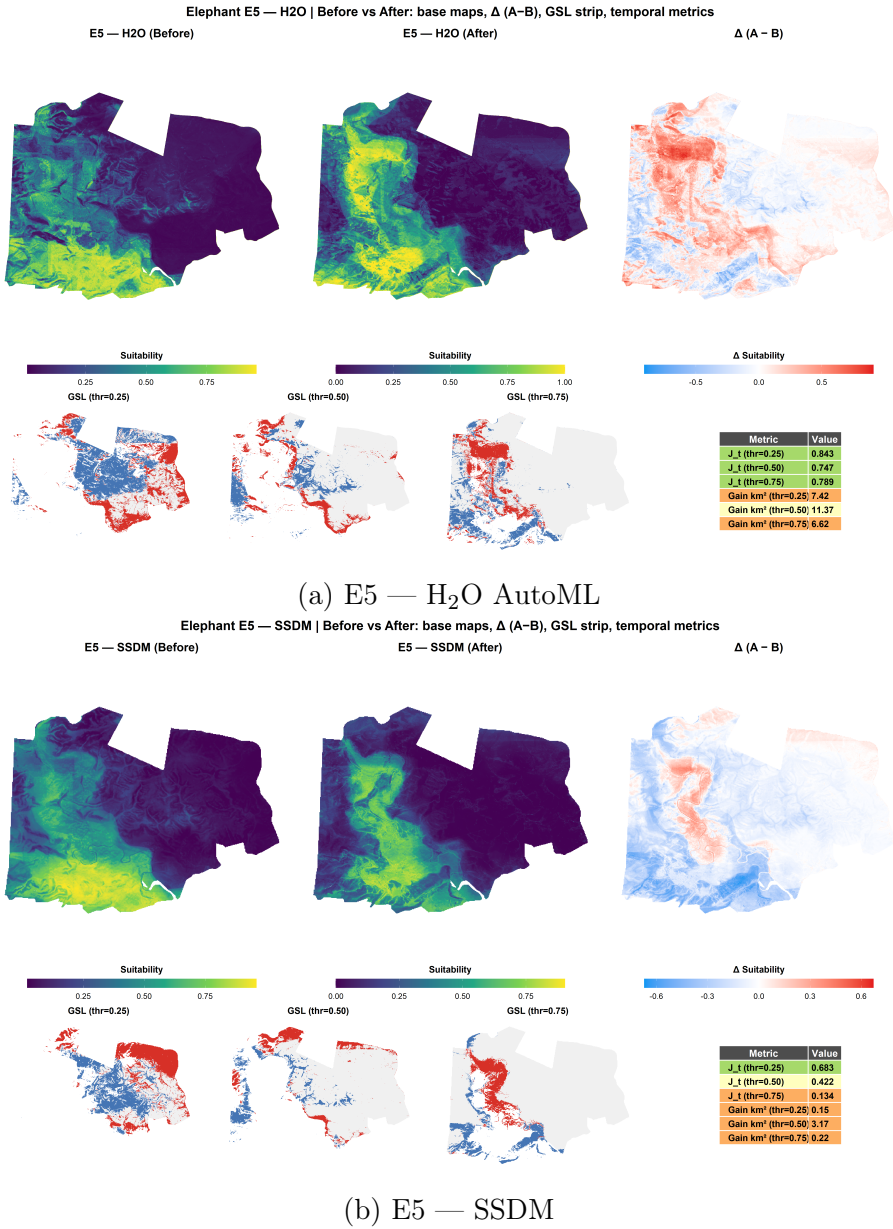
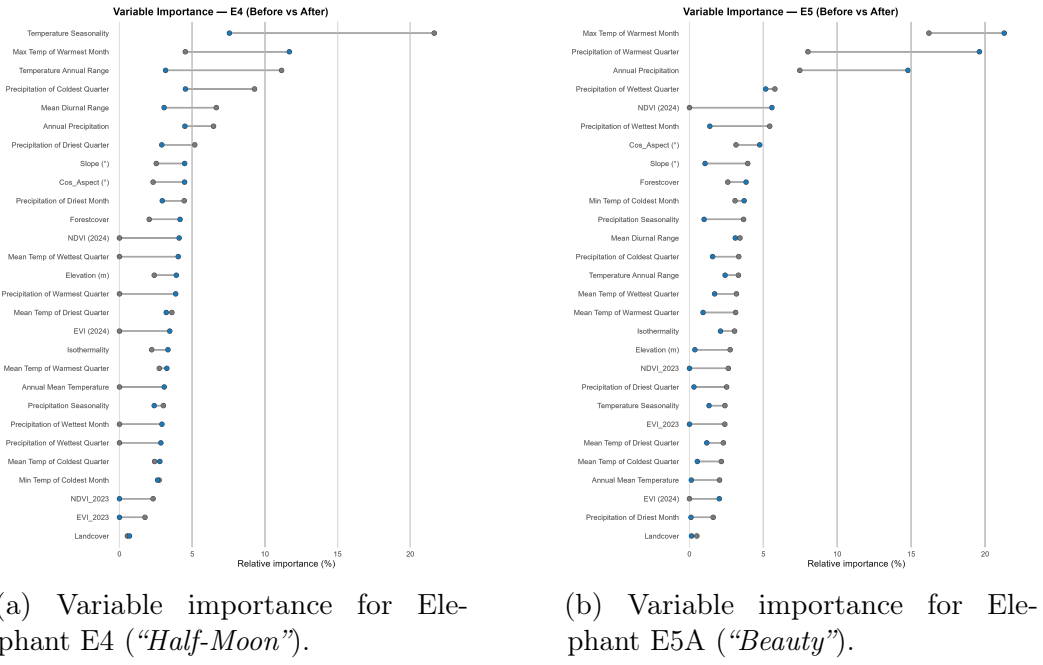


Figure 13: Per-elephant comparison for Beauty (E5). Stacked panels show vertical alignment of H<sub>2</sub>O AutoML (top) and SSDM (bottom) results for clearer visual comparison of habitat change.



(a) Variable importance for Elephant E4 ("Half-Moon").

(b) Variable importance for Elephant E5A ("Beauty").

Figure 14: Variable importance comparisons for the female elephants E4 ("Half-Moon") and E5A ("Beauty") under the AutoML and SSDM frameworks.

## 1006 6.2 H<sub>2</sub>O AutoML Results (After Fence Removal)

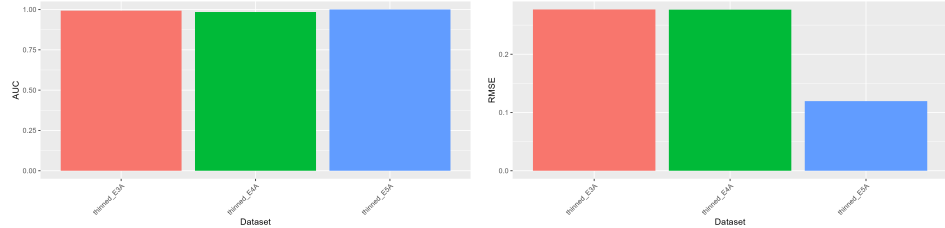


Figure 15: Model performance summary (After): AUC and RMSE across elephants.

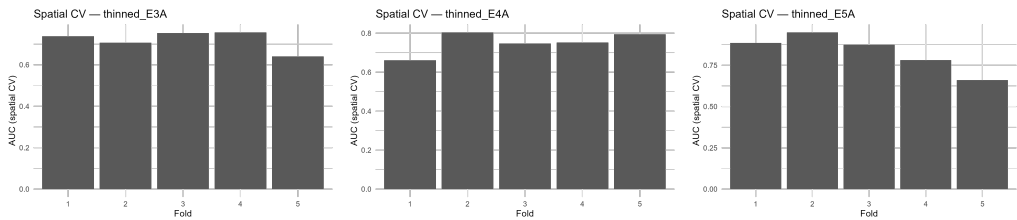


Figure 16: Spatial block cross-validation AUC for individual elephants (After).

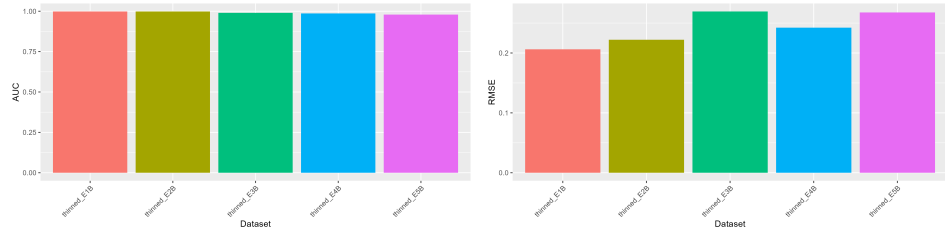


Figure 17: Model performance summary (Before): AUC and RMSE across elephants.

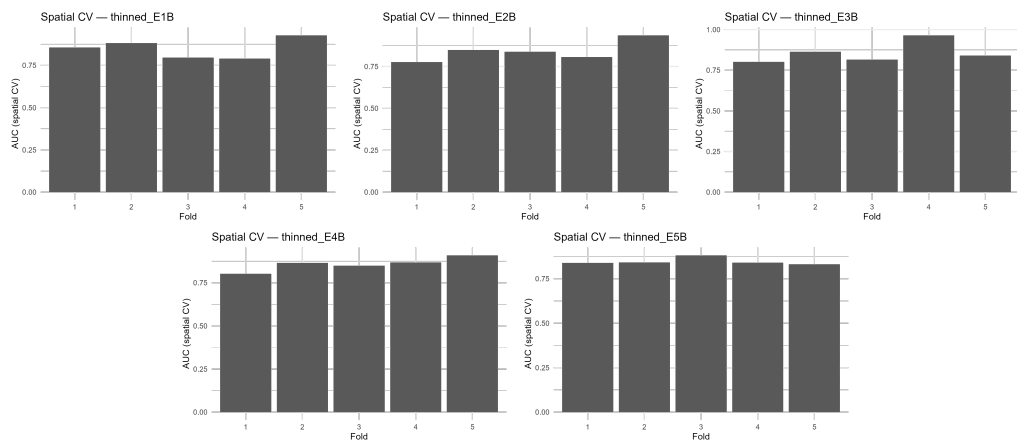
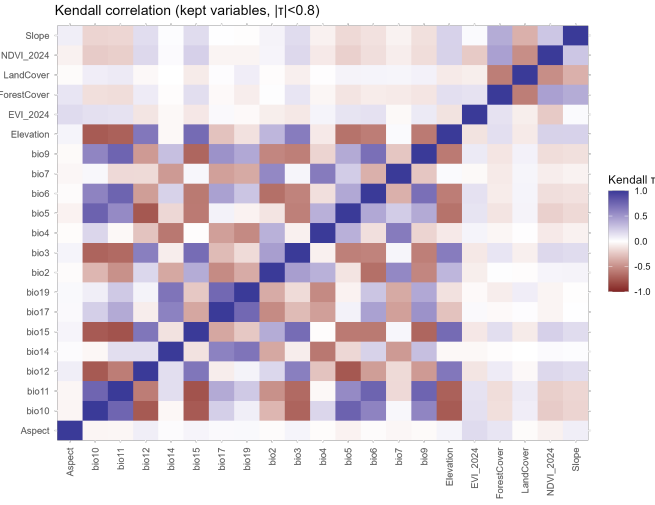
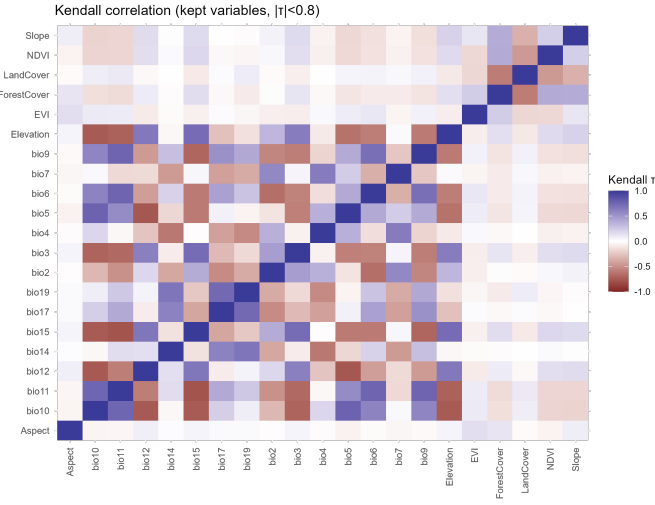


Figure 18: Spatial block cross-validation AUC for individual elephants (Before).



(a) After fence removal (Set A).



(b) Before fence removal (Set B).

Figure 19: Kendall's  $\tau$  correlation heatmaps of retained environmental predictors. The upper panel shows variable relationships for the post-fence (After) period, while the lower panel represents pre-fence (Before) conditions. Predictors exceeding  $\tau > 0.8$  were excluded to minimize multicollinearity.

1007 **6.3 Base Learner Contributions**

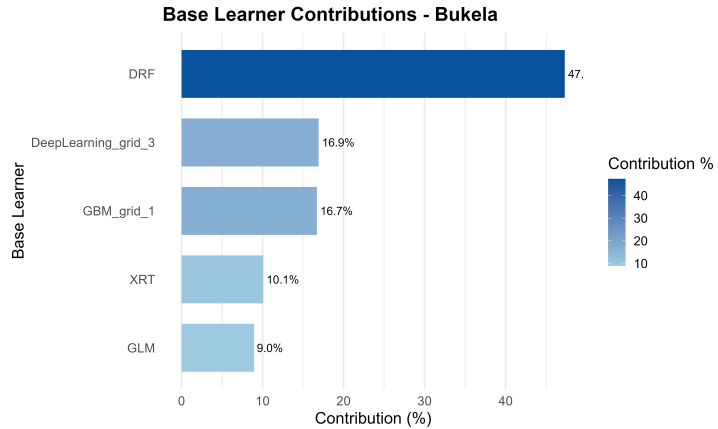


Figure 20: E3A — Bukela

1008 Base learner contributions demonstrate how stacked models combine al-  
1009 gorithms to achieve improved accuracy. Figure 22 shows each base learner's  
1010 contribution. In E3A, XRT contributed 35%, GBM 23.1%, DeepLearning  
1011 16.2%, DRF 15.6%, and GLM 9.7%, showing strong reliance on tree-based  
1012 methods. E4A was led by DeepLearning\_grid\_2 (35%), DRF (23.1%), and  
1013 DeepLearning\_grid\_1 (18.2%), while GBM and GLM contributed less, sug-  
1014 gesting E4A required more complex nonlinear structures to capture elephant  
1015 habitat dynamics.

1016 **6.4 End-to-end reproducibility**

1017 All workflows—from data processing and spatial analysis to species distribu-  
1018 tion modelling, ensemble construction, and visualisation—are scripted and

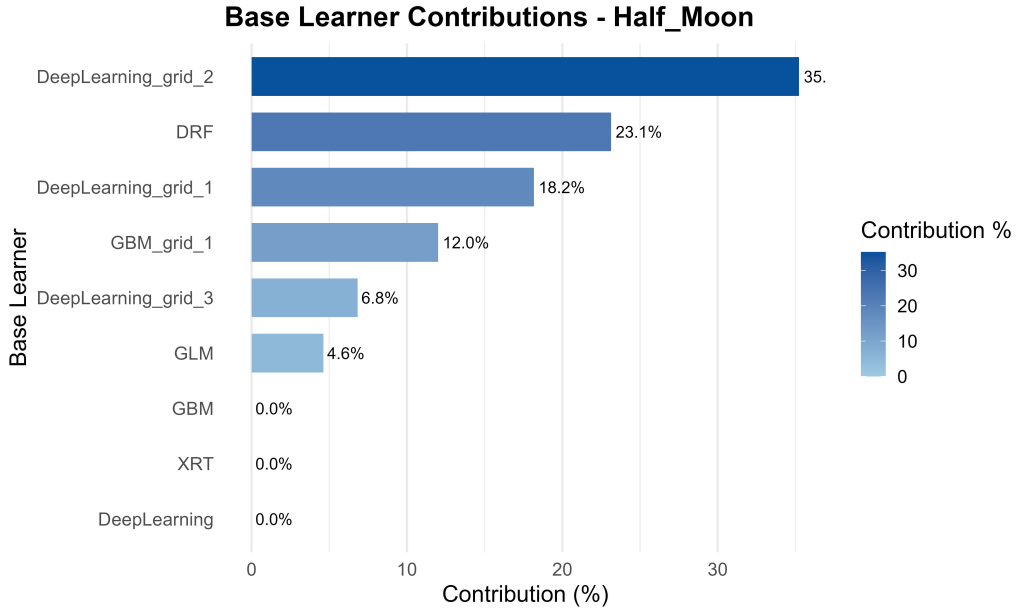


Figure 21: E4A — Half Moon

Figure 22: Base learner contributions for H<sub>2</sub>O AutoML ensemble models. Each bar plot shows the relative weight of individual algorithms (e.g., GBM, DRF, XGBoost, Deep Learning) contributing to the final stacked ensemble for two elephants (E3A and E4A).

1019 versioned. Documentation is provided in `README.md` and code base, hosted  
 1020 on GitHub ([https://github.com/\[your-repo\]](https://github.com/[your-repo])). Computational time was  
 1021 logged per model (Appendix X). Results were generated in REPRO mode to  
 1022 mitigate stochastic randomness. The `renv.lock` ensures strict replicability  
 1023 of software environment, code, and package versions for exact reproduction.  
 1024 Workflows, input data, and post-processing scripts are available, making the  
 1025 research process transparent and repeatable.

1026 **6.5 Ethical use of AI**

1027 This research adheres to ethical AI standards, consistent with Elsevier guide-  
1028 lines. No images were generated or manipulated using AI. The first author  
1029 takes full responsibility for research accuracy and ethical standards. AI  
1030 tools (*SciSpace*, *Perplexity*, *Quillbot*) were used for improving language and  
1031 readability, while code assistants (*ChatGPT*, *Perplexity AI*) reduced script  
1032 redundancy and automated R programming, not for data analysis or interpre-  
1033 tation. All substantive decisions, analyses, and interpretations remain strictly  
1034 those of the authors. AI-generated content was assessed using *SciSpace AI*  
1035 *Detector*, with detected AI content below 10% (score: 1%). No sensitive,  
1036 proprietary, or personal data was uploaded to external AI services.

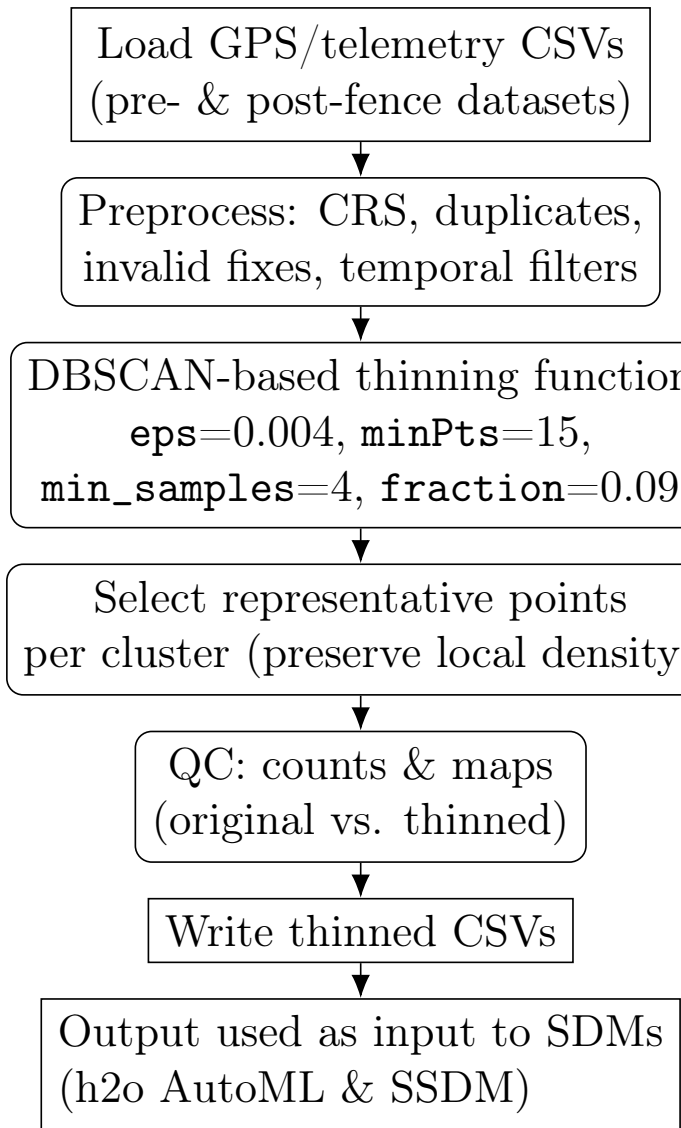


Figure 23: DBSCAN-based thinning workflow used to reduce spatial auto-correlation and computational load while preserving local density patterns. Parameters were tuned empirically (`eps=0.004`, `minPts=15`, `min_samples=4`, `fraction=0.09`).